Inorganic Chemistry
DOI: 10.1021/acs.inorgchem.6b02409

Bifunctional chalcogen linkers for the stepwise generation of multimetallic assemblies and functionalized nanoparticles.

Jonathan A. Robson,[a+] Ferran Gonzàlez de Rivera,[a,b+] Khairil A. Jantan,[a] Margot. N. Wenzel,[a] Andrew J. P. White,[a] Oriol Rossell,[b] and James D. E. T. Wilton-Ely[a*]

[a]*Department of Chemistry, Imperial College London, South Kensington Campus, London SW7 2AZ (UK).* [b]*Departament de Química Inorgànica, Universitat de Barcelona, Martí Franquès 1-11, 08028, Barcelona, Spain. E-mail: j.wilton-ely@imperial.ac.uk*

[+] These authors contributed equally.

Supporting Information (consisting of TEM, EDS, TGA data for **NP1** – **NP4**, selected NMR spectra, details of the Signer molecular mass determination apparatus and crystallographic data for **21**) is available on the WWW at http://.

Keywords: ruthenium, gold, thiolate, carboxylate, nanoparticles

Abstract

The disulfide ligand, $(SC_6H_4CO_2H\text{-}4)_2$, acts as a simple but versatile linker for a range of group 8 transition metals through reaction of the oxygen donors. This leads to a range of homobimetallic ruthenium and osmium alkenyl compounds $[\{M(CH{=}CHR)(CO)(PPh_3)_2(O_2CC_6H_4S\text{-}4)\}_2]$ (M = Ru, Os; R = C_6H_4Me-4). Additional metal-based functionality can be added through the use of precursors incorporating rhenium bipyridine units (R = bpyReCl$(CO)_3$). The more robust disphosphine ligands in $[\{Ru(dppm)_2(O_2CC_6H_4S\text{-}4)\}_2]^{2+}$ (dppm = diphenylphosphinomethane) allow reduction of the disulfide bond with sodium borohydride to yield the thiol complex, $[Ru(O_2CC_6H_4SH\text{-}4)(dppm)_2]^{+}$. This complex reacts with $[AuCl(PPh_3)]$ to afford the bimetallic compound, $[Ru(dppm)_2(O_2CC_6H_4S\text{-}4)Au(PPh_3)]^{+}$. However, an improved route to the same and related heterobimetallic compounds is provided by the reaction of *cis*-$[RuCl_2(dppm)_2]$ with $[Au(SC_6H_4CO_2H\text{-}4)(L)]$ (L = PPh_3, PCy_3, PMe_3, IDip) in the presence of base and NH_4PF_6 (IDip = 1,3-bis(2,6-diisopropylphenyl)imidazol-2-ylidene). The heterotrimetallic compound $[Au(SC_6H_4CO_2Ru(dppm)_2)_2]^{+}$ is accessible through the reaction of homoleptic gold(I) dithiolate $[Au(SC_6H_4CO_2H\text{-}4)_2]$PPN (PPN = bis(triphenylphosphine)iminium) with *cis*-$[RuCl_2(dppm)_2]$. Without departing from the same methodology, greater complexity can be incorporated into the system to provide the penta- and heptametallic assembles $[(dppf)\{AuSC_6H_4CO_2Ru(dppm)_2\}_2]^{2+}$ and $[(dppf)\{AuSC_6H_4CO_2Os(CH{=}CH\text{-}bpyReCl(CO)_3)(CO)(PPh_3)_2\}_2]$. The same stepwise approach provides the dinuclear, organometallic complexes, $[(L)Au(SC_6H_4CO_2\text{-}4)M(CH{=}CHC_6H_4Me\text{-}4)(CO)(PPh_3)_2]$ (M = Ru, Os; L = PPh_3, IDip). Complexes containing three metals from different groups $[(L)Au(SC_6H_4CO_2\text{-}4)M\{CH{=}CH\text{-}bpyReCl(CO)_3\}(CO)(PPh_3)_2]$ (M = Ru, Os) can also be prepared with one ruthenium example (L = PPh_3) being structurally characterised. In order to illustrate the versatility of this approach, the synthesis and characterization (IR, NMR spectroscopies, TEM, EDS and TGA) of the functionalized gold and palladium nanoparticles $Au@[SC_6H_4CO_2Ru(dppm)_2]^{+}$ and $Pd@[SC_6H_4CO_2Ru(dppm)_2]^{+}$ is reported.

Introduction

The incorporation of multiple metal centers within the same assembly, whether molecular or nanoscale in nature, opens up new possibilities in a variety of applications. The potential for multisite interactions, cooperative effects and higher localized density of metal sites has been exploited in sensing,[1] imaging,[2] and catalysis.[3] In the latter field, additional motivation has come from the presence of bimetallic systems in nature.[4] The linking of organometallic compounds with (often highly conjugated) organic linkers, such as acetylides, has also led to the exploration of novel spectroscopic and photophysical properties.[5]

While the preparation of multimetallic compounds and materials consisting of the same metal has been exploited extensively in areas such as metal-organic frameworks (MOFs)[6a-c] and coordination polymers,[6d,e] access to heteromultimetallic systems has always proved more challenging due to the need for strategies suited to linking different metals together in a consistent and controllable manner. While protection/deprotection approaches offer a solution to this problem, an alternative, more synthetically straightforward option is to tailor bifunctional linkers to the metals involved (Chart 1). This approach has been used by us[7] and others[8] to access molecular assemblies consisting of between two and six metals, encompassing compounds in which up to six different metals are combined.[8c]

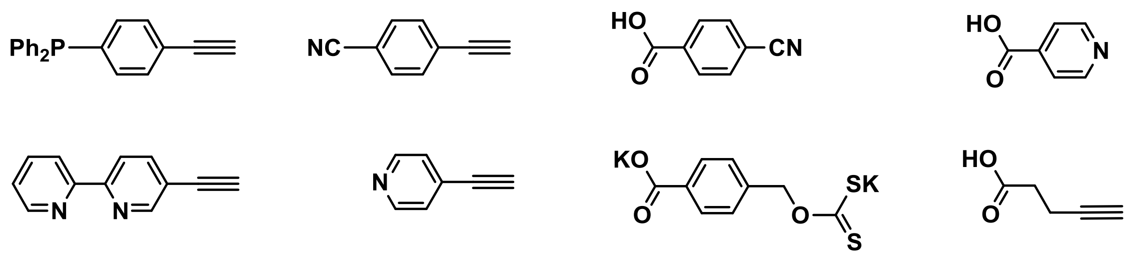

Chart 1. Simple bifunctional ligands used in the construction of multimetallic assemblies.

In our earlier studies,[9] sulfur ligands have dominated due to their utility in both molecular and nanoparticle systems. These approaches have been based principally on the versatile dithiocarbamate ligand class, which can be introduced at a late stage in the assembly of the systems in order to avoid undesired reactivity with the molecular metal unit ('backbiting'). Due to this potential problem, the use of thiols as a donor component of bifunctional linkers is usually avoided in systems containing 'soft' metal centers. However, in this contribution, the reactivity of 4-mercaptobenzoic acid is explored, both in thiolate and disulfide form. The differing reactivity of sulfur and oxygen donors and the lower reactivity of the disulfide linkage allow the preparation of heteromultimetallic compounds based on Re, Ru, Os and Au as well as the surface functionalization of gold and palladium nanoparticles.

In order to illustrate the potential for wide-ranging application of this approach, a series of different metal units were employed. These included representatives of common geometries and a range of metals from groups 7, 8 and 11 from all three periods of the d-block. In addition, the metal units chosen also possess properties, which are widely employed in many applications, such as reliable redox behaviour [(Fe(II/III), Ru(II/III)], photophysical attributes (Re(I)-diimine moieties) or a common motif used in gold-based drugs (e.g., auranofin).

Results and Discussion

Synthesis of multimetallic complexes

Reaction of 4-mercaptobenzoic acid with iodine provided the disulfide $(SC_6H_4CO_2H\text{-}4)_2$ (**1**) as a colorless solid in almost quantitative yield. The absence of the thiol resonance observed in the ^{1}H NMR spectrum of the precursor and a slight shift in the chemical shift values of the aryl resonances (7.52 and 7.81 ppm, J_{HH} = 8.0 Hz) indicated the success of the reaction. Remaining spectroscopic and analytical data agreed with those reported for this compound previously.[10] Treatment of two equivalents of the versatile precursor, *cis*-$[RuCl_2(dppm)_2]$, with **1** in the presence of sodium methoxide and NH_4PF_6 resulted in formation of a pale yellow solid in 86% yield (Scheme 1). Two new pseudotriplet resonances in the $^{31}P\{^1H\}$ NMR spectrum at −12.0 and 8.9 ppm (J_{PP} = 39.0 Hz) indicated the formation of a new compound. ^{1}H NMR analysis revealed features attributed to the dppm ligands, such as multiplets due to the PCH_2P protons at 3.95 and 4.63 ppm, while the resonances for the C_6H_4 protons were obscured by the remaining aromatic features of the spectrum. In the $^{13}C\{^1H\}$ NMR spectrum, a triplet at 43.6 (J_{PC} = 11.5 Hz) ppm was assigned to the bridgehead carbon nuclei of the dppm ligands, while a singlet at 181.7 ppm was attributed to the CO_2 unit. The formulation of $[\{Ru(dppm)_2(O_2CC_6H_4S\text{-}4)\}_2](PF_6)_2$ (**2**) was further supported by a molecular ion at *m/z* 2044 in the mass spectrum (FAB, positive mode) and good agreement between calculated and experimentally determined values for elemental composition.

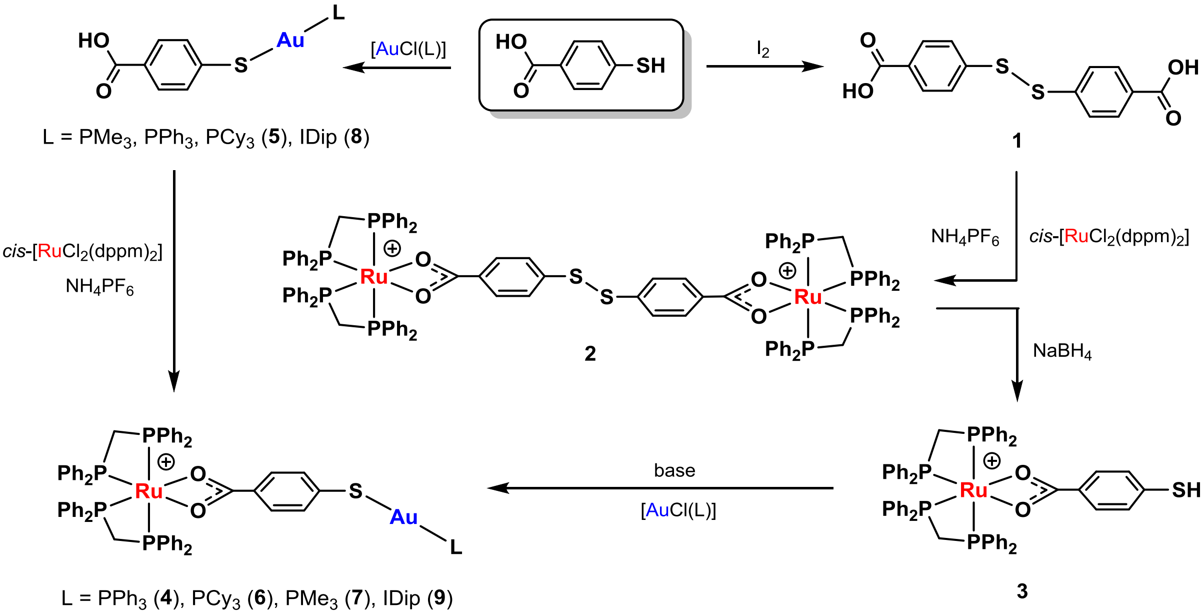

Scheme 1. Synthesis of bi- and trimetallic complexes. All charged complexes are hexafluorophosphate salts.

In order to add a second metal unit to **2**, scission of the disulfide bond was necessary. However, this had to be performed under conditions which were tolerated by the Ru(dppm)$_2$ moieties. After attempting this transformation unsuccessfully with tri(*n*-butyl)phosphine, it was found that sodium borohydride was able to achieve the transformation to the corresponding thiol, [Ru(O$_2$CC$_6$H$_4$SH-4)(dppm)$_2$]PF$_6$ (**3**). However, the NMR data were found to be only slightly shifted from those for the precursor (**2**) and the presence of the thiol proton was initially difficult to identify. Mass spectrometry data (ES, positive mode) supported the formation of the desired product with a molecular ion at *m/z* 1024. The Signer osmometry method was also employed, which estimates molecular mass based on vapor pressure values compared to a known standard (Supporting Information).[11] Data obtained by this method were also found to support the monometallic formulation. Further proof was provided through reactivity studies with gold(I) phosphine complexes. While reaction of compound **2** with [AuCl(PPh$_3$)] in the presence (or absence) of base failed to yield a reaction, treatment of **3** with the same gold(I) reagent in the presence of base led to formation of the complex [(dppm)$_2$Ru(O$_2$CC$_6$H$_4$S-4)Au(PPh$_3$)]PF$_6$ (**4**). A new resonance at 38.5 ppm in the ^{31}P{^{1}H} NMR spectrum indicated the presence of the new triphenylphosphine ligand in the product, as did the presence of additional resonances in the ^{13}C{^{1}H} NMR spectrum for the AuPPh$_3$ unit. The mass spectrum (ES, positive mode) showed a molecular ion at *m/z* 1481. In order to further confirm the identity of the product, the known compound, [Au(SC$_6$H$_4$CO$_2$H-

4)(PPh_3)],[12a] was treated with *cis*-[$RuCl_2$($dppm)_2$], NaOMe and NH_4PF_6 to provide an alternative and higher yield route to **4** (Scheme 1).

This result, and also the chemospecific nature of the reaction, led to investigation of the reaction of other related gold(I) precursors with *cis*-[$RuCl_2$($dppm)_2$]. The new thiolate compound, [Au($SC_6H_4CO_2H$-4)(PCy_3)] (**5**), was prepared from [AuCl(PCy_3)] and $HSC_6H_4CO_2H$-4 in the presence of base. This was then used to prepare [($dppm)_2$Ru($O_2CC_6H_4S$-4)Au(PCy_3)]PF_6 (**6**) in the same way employed for **4**. The presence of three resonances in the $^{31}P\{^1H\}$ NMR spectrum at −12.1 (dppm), 8.9 (dppm) and 57.6 (PCy_3) ppm confirmed the presence of the ruthenium and gold phosphine units at either end of the mercaptobenzoate linker. An abundant molecular ion in the mass spectrum (ES, positive mode) at *m/z* 1500 confirmed this formulation. Using the same method, [($dppm)_2$Ru($O_2CC_6H_4S$-4)Au(PMe_3)]PF_6 (**7**) was also synthesized from [AuCl(PMe_3)] (Scheme 1).

In order to extend the use of gold fragments beyond [$AuPR_3$]$^+$ units, the new complex [Au($SC_6H_4CO_2H$-4)(IDip)] (**8**) was prepared from the NHC precursor, [AuCl(IDip)] (IDip = 1,3-bis(2,6-diisopropylphenyl)imidazol-2-ylidene). Compound **8** was treated with base and *cis*-[$RuCl_2$($dppm)_2$] to provide [($dppm)_2$Ru($O_2CC_6H_4S$-4)Au(IDip)]PF_6 (**9**) in 62% yield (Scheme 1). The integration between the resonances for the methylene protons of the dppm ligands (3.89 and 4.63 ppm) and the methyl substituents on the NHC ligand (four doublets between 1.25 and 1.44 ppm) provided evidence for the formulation, as well as mass spectrometry and analytical data. Similar reactions were attempted with the complexes [Au($SC_6H_4CO_2H$-4)(CNR)] (R = ^{t}Bu, ^{i}Pr),[12b] however, the isocyanide ligand proved less robust than the NHC analogues and was partially lost, leading to a mixture of intractable products.

The homoleptic gold(I) dithiolate species, [Au($SC_6H_4CO_2H$-4$)_2$]PPN (PPN = bis(triphenylphosphine)iminium),[12a] was treated with *cis*-[$RuCl_2$($dppm)_2$] and base (Scheme 2) to afford the trimetallic compound [Au{$SC_6H_4CO_2Ru(dppm)_2$}$_2$]PF_6 (**10**). Analysis by ^{31}P and ^1H NMR spectroscopy revealed chemical shifts displaying little difference to those of the resonances in compound **2**. Bearing in mind the possible effect the P(III) and P(V) oxidation states could exert on the relaxation times of the relevant phosphorus nuclei, integration of the $^{31}P\{^1H\}$ NMR spectrum suggested a dppm:PF_6^- ratio of 8:1, indicating a single counteranion for the complex. Mass spectrometry data for the precursor, [Au($SC_6H_4CO_2H$-4$)_2$]PPN revealed a molecular ion, however, in the spectrum of **10**, only an abundant fragmentation for loss of gold was observed. The overall formulation was confirmed by good agreement of elemental analysis with calculated values.

Using the known compound, $[dppf(AuSC_6H_4CO_2H\text{-}4)_2]$ (dppf = 1,1’-diphenylphosphinoferrocene),[12a] a heteropentametallic $FeRu_2Au_2$ compound, $[(dppf)\{AuSC_6H_4CO_2Ru(dppm)_2\}_2](PF_6)_2$ (**11**), was prepared in 61% yield (Scheme 2). The presence of the cyclopentadienyl rings was indicated by the observation of resonances at 4.24 and 4.63 ppm in the ^1H NMR spectrum alongside typical features for the PCH_2P and aromatic protons. Support for the overall composition was provided by MALDI mass spectrometry (*m/z* 3031 for $[M + K]^+$) and good agreement of elemental analysis with calculated values.

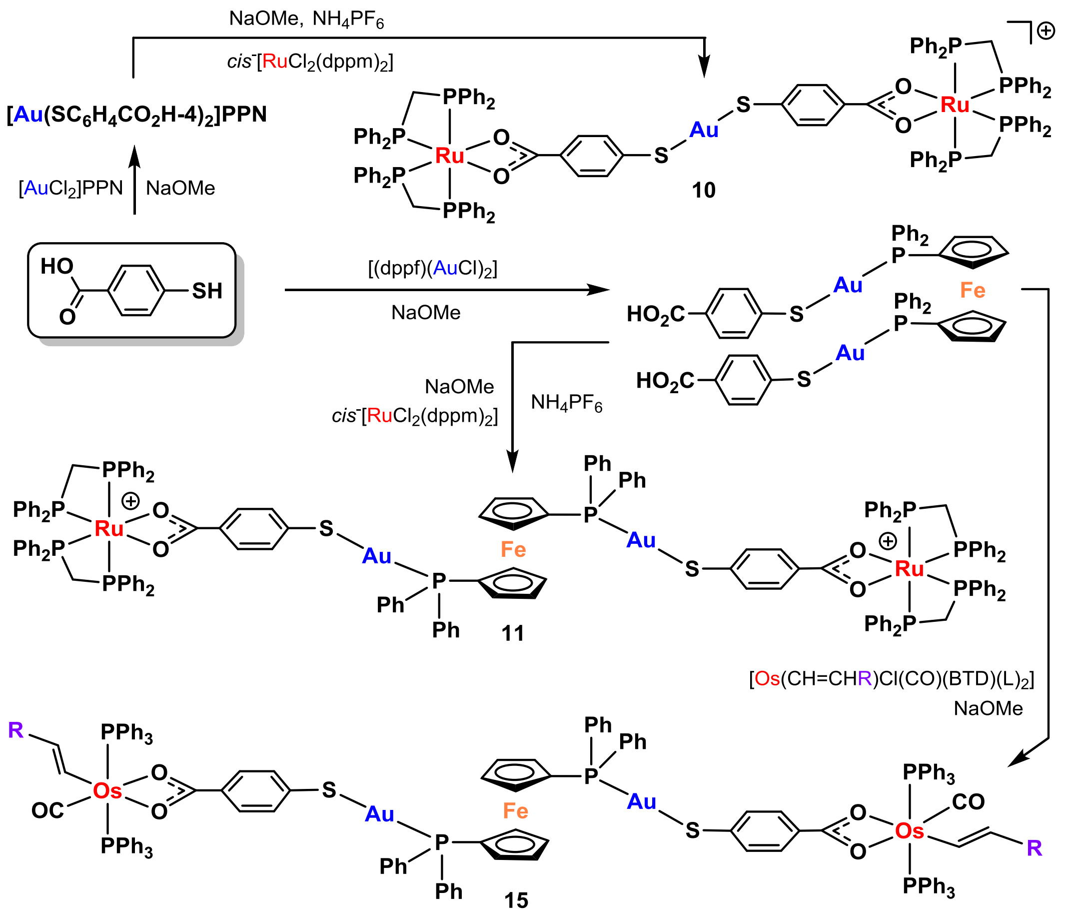

Scheme 2. Synthesis of a penta- and heptametallic complexes; R = $bpyReCl(CO)_3$, L = PPh_3, BTD = 2,1,3-benzothiadiazole, PPN = bis(triphenylphosphino)iminium. All metal cations are hexafluorophosphate salts.

The $Ru(dppm)_2$ unit is ideal for use in applications where a robust terminus with characteristic spectroscopic features (^1H, $^{31}P\{^1H\}$ NMR) is required. However, the potential for subsequent functionalization is mainly limited to exchange of the counteranion. A more versatile synthetic starting point is provided by group 8 vinyl complexes,[13] such as

$[M(CR{=}CHR')Cl(CO)(BTD)(PPh_3)_2]$ (M = Ru,[14] Os;[15] BTD = 2,1,3-benzothiadiazole). These complexes are readily accessible from the hydride precursors, $[MHCl(CO)(BTD)(PPh_3)_2]$, by alkyne hydrometalation. This allows further functionality (including metal centers) to be introduced through the choice of alkyne substituent. This has been exploited to prepare bimetallic systems[16] and to incorporate fluorophores for use in carbon monoxide sensing.[17] In addition, the resultant vinyl complexes, $[M(CR{=}CHR')Cl(CO)(BTD)(PPh_3)_2]$, possess labile ligands (BTD, chloride, phosphine) enabling the reactivity at the metal center to be exploited, which has been the focus of our earlier studies.[18] This potential has been harnessed by us[7a,9c,18h] and others[19] to bridge such metal centers. It was thus decided to extend the investigation of multimetallic compound generation in this work through both the vinyl ligand and the substitution of labile ligands.

Addition of carboxylic acids to ruthenium vinyl complexes can lead to cleavage of the organic ligand to yield the corresponding alkene.[7b] However, this can be avoided if deprotonation is achieved prior to addition of the vinyl complex. Treatment of $[Ru(CH{=}CHC_6H_4Me\text{-}4)Cl(CO)(BTD)(PPh_3)_2]$ with disulfide **1** in the presence of base led to the formation of a new compound which gave rise to a singlet in the $^{31}P\{^1H\}$ NMR spectrum at 37.7 ppm, indicating a mutually *trans* arrangement of phosphines and the highly symmetrical nature of the complex. The coordination of the oxygen donors in preference to the sulfur unit was provided by a shift in frequency for the $\nu_{C=O}$ absorption from 1676 cm^{-1} in **1** to 1575 cm^{-1} in the product. Evidence for retention of the tolylvinyl ligand was provided by resonances in the ^1H NMR spectrum for the α and β protons at 7.82 and 5.85 ppm, showing a mutual coupling of 15.5 Hz. In comparison to the complexes bearing the dppm ligand, the aromatic region was sufficiently simplified to identify the protons of the SC_6H_4 unit as an AA'BB' system at 7.05 and 7.10 ppm (J_{HH} = 8.6 Hz). Characteristic resonances were observed for the carbonyl ligand at 202.4 (t, J_{PC} = 11.3 Hz) ppm and the CO_2 unit at 176.4 ppm in the $^{13}C\{^1H\}$ NMR spectrum. On the basis of these data and those from mass spectrometry and elemental analysis measurements, the complex was formulated as the bimetallic complex, $[\{Ru(CH{=}CHC_6H_4Me\text{-}4)(CO)(PPh_3)_2(O_2CC_6H_4S\text{-}4)\}_2]$ (**12**). The osmium analogue, $[\{Os(CH{=}CHC_6H_4Me\text{-}4)(CO)(PPh_3)_2(O_2CC_6H_4S\text{-}4)\}_2]$ (**13**), was prepared in a similar fashion (Scheme 3) and displayed very similar spectroscopic data to **12** apart from an upfield shifted resonance in the $^{31}P\{^1H\}$ NMR spectrum at 18.5 ppm and a lower frequency ν_{CO} absorption at 1906 cm^{-1}. The potential for introducing further metal fragments through the vinyl ligand was illustrated by the use of $[ReCl(CO)_3(bpyC{\equiv}CH)]$, which has previously been used by Lang and co-workers to form acetylide complexes of various metals.[8a-i] It appeared that its potential in hydroosmiation reactions has been overlooked until the preparation of [{Os{CH=CH-bpyReCl$(CO)_3$}(CO)(BTD)$(PPh_3)_2$] through insertion of this alkyne into the Os-H bond of [OsHCl(CO)(BTD)$(PPh_3)_2$].[7a] Treatment of two equivalents of this ReOs bimetallic product with **1** in the presence of base yielded [{Os{CH=CH-bpyReCl$(CO)_3$}(CO)$(PPh_3)_2$($O_2CC_6H_4S$-4)}$_2$] (**14**). The presence of the rhenium unit was indicated by resonances at 9.36 (Hα) and 5.72 (Hβ) ppm in the ^{1}H NMR spectrum for the new vinyl ligand showing mutual coupling of 16.2 Hz. The additional activity in the solid state infrared spectrum between 1882 and 2015 cm^{-1} was attributed to the carbonyl ligands attached to the rhenium center. The tetrametallic nature of the compound (Scheme 3) was further supported by mass spectrometry and analytical data. Spurred on by this result, the strategy employed to prepare **11** was revisited using [{Os{CH=CH-bpyReCl$(CO)_3$}(CO)(BTD)$(PPh_3)_2$] and [dppf($AuSC_6H_4CO_2$-4)$_2$] in the presence of base (Scheme 2). The complex formed, [(dppf){$AuSC_6H_4CO_2$Os(CH=CH-bpyReCl$(CO)_3$)(CO)$(PPh_3)_2$}$_2$] (**15**), possesses seven metals ($Re_2FeOs_2Au_2$) and was initially characterized based on the highly diagnostic ^{1}H NMR spectrum. Each structural unit provided characteristic resonances, including the dppf (4.30, 4.64 ppm), SC_6H_4 (6.89 and 7.25 ppm), bpy (e.g., 7.75 and 7.92 ppm) and vinyl (5.63 and 9.38 ppm) moieties. Further support for the structure came from the other analytical and spectroscopic techniques employed.

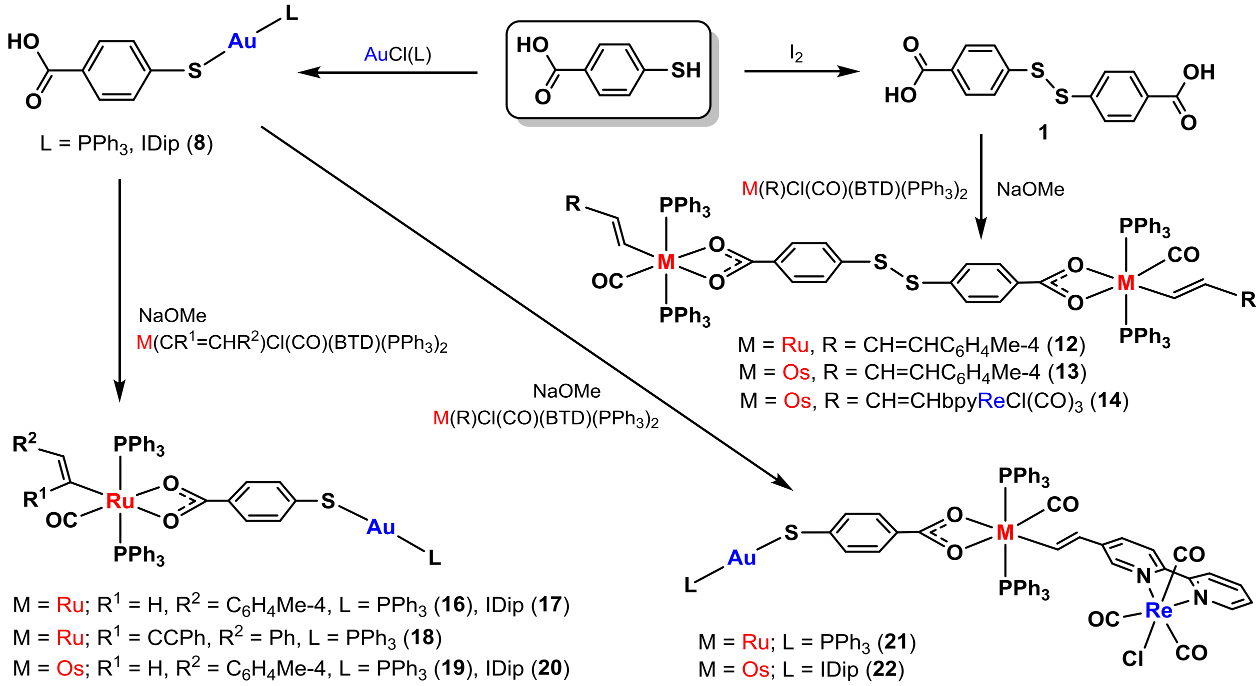

Scheme 3. Synthesis of bi- and trimetallic vinyl complexes; BTD = 2,1,3-benzothiadiazole.

The complex $[Au(SC_6H_4CO_2\text{-}4)(PPh_3)]$[12a] was used to prepare the heterobimetallic complex, $[(Ph_3P)Au(SC_6H_4CO_2\text{-}4)Ru(CH{=}CHC_6H_4Me\text{-}4)(CO)(PPh_3)_2]$ (**16**), bearing the tolylvinyl ligand. The NHC compound $[Au(SC_6H_4CO_2\text{-}4)(IDip)]$ (**8**) was employed to prepare the NHC analogue $[(IDip)Au(SC_6H_4CO_2\text{-}4)Ru(CH{=}CHC_6H_4Me\text{-}4)(CO)(PPh_3)_2]$ (**17**), in which organometallic ligands are present at either end of the carboxylate-thiolate linker. Using the 5-coordinate enynyl compound, $[Ru(C(C{\equiv}CPh){=}CHPh)Cl(CO)(PPh_3)_2]$, an example bearing a disubstituted alkenyl ligand, $[(Ph_3P)Au(SC_6H_4CO_2\text{-}4)Ru(C(C{\equiv}CPh){=}CHPh)(CO)(PPh_3)_2]$ (**18**), was prepared.

The osmium analogues, $[(Ph_3P)Au(SC_6H_4CO_2\text{-}4)Os(CH{=}CHC_6H_4Me\text{-}4)(CO)(PPh_3)_2]$ (**19**) and $[(IDip)Au(SC_6H_4CO_2\text{-}4)Os(CH{=}CHC_6H_4Me\text{-}4)(CO)(PPh_3)_2]$ (**20**), were also prepared in a similar manner to yield two examples of OsAu heterobimetallic complexes. These syntheses paved the way for the preparation of two heterotrimetallic complexes with metals drawn from groups 7, 8 and 11 of the periodic table. Treatment of $[Au(SC_6H_4CO_2\text{-}4)(L)]$ (L = PPh_3, IDip) with $[\{M\{CH{=}CH\text{-}bpyReCl(CO)_3\}(CO)(BTD)(PPh_3)_2]$ (M = Ru, Os) and NaOMe led to formation of $[(L)Au(SC_6H_4CO_2\text{-}4)M\{CH{=}CH\text{-}bpyReCl(CO)_3\}(CO)(PPh_3)_2]$ (M = Ru, L = PPh_3 **21**; M = Os, L = IDip **22**). While a number of features in complex **22** were obscured by features due to the PPh_3 ligands, resonances for both metal units were observed in the ^1H NMR spectrum. These included resonances for the

Hα (9.43 ppm) and Hβ (5.64 ppm) protons of the vinyl ligand and the methyl groups of the IDip ligands at 1.30, 1.35 (both doublets) and 2.66 (septet) ppm. As before, the overall composition was supported by elemental analysis data and the presence of a molecular ion at *m/z* 1967 in the mass spectrum (ES, positive mode). To the best of our knowledge, **22** represents the first example of a molecular trimetallic assembly incorporating Re, Os and Au.

Numerous attempts were made using many different techniques (vapor diffusion, layering, slow evaporation etc.) and solvent combinations to obtain crystals of the key complexes reported here. Ultimately, single crystals suitable for structural determination were grown through slow diffusion of ethanol into a dichloromethane solution of complex **21** (Figure 1).

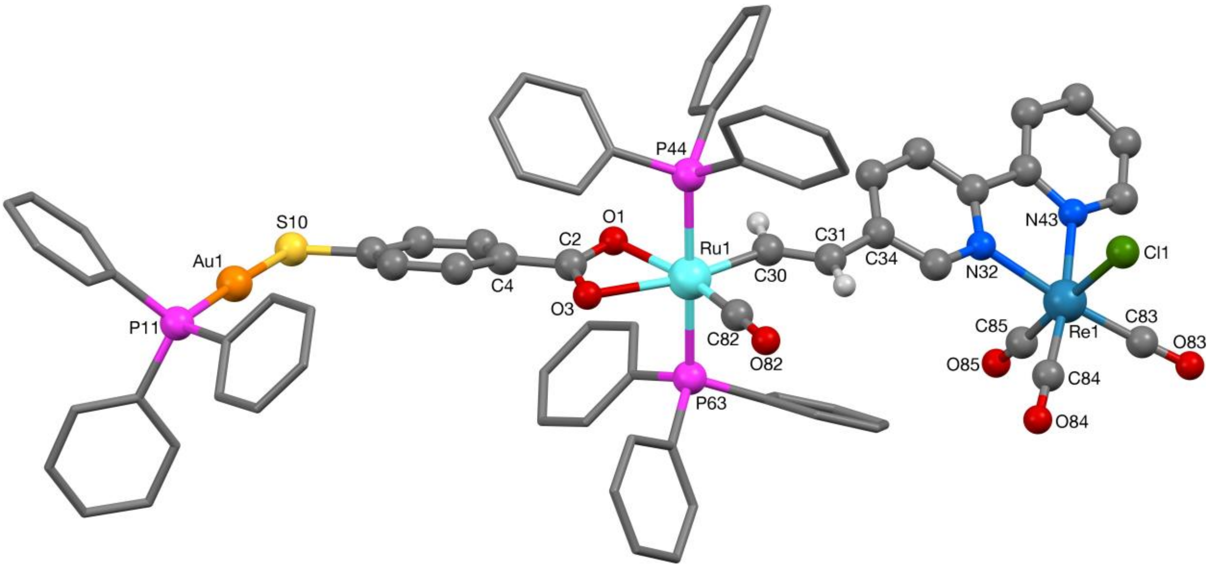

Figure 1. The molecular structure of **21**. Selected bond lengths (Å) and angles (°); Au1–S10 2.303(2), Au1–P11 2.255(2), Re1–N32 2.176(5), Re1–N43 2.162(5), Ru1–O1 2.191(4), Ru1–O3 2.233(4), Ru1–C30 2.010(5), Ru1–P44 2.381(2), Ru1–P63 2.376(2), S10–Au1–P11 176.39(6), N32–Re1–N43 74.5(2), O1–Ru1–O3 59.2(2), P44–Ru1–P63 176.31(6), Ru1–C30–C31 136.0(5).

The structure of the ReRuAu trimetallic complex [$(Ph_3P)Au(SC_6H_4CO_2$-4)Ru{CH=CHbpyReCl$(CO)_3$}(CO)$(PPh_3)_2$] (**21**) can be discussed in relation to previously reported structural data for the individual metal units. The bond data for the common distorted octahedral motif, [ReCl$(CO)_3$(bpy)], are unremarkable and are similar to those for the precursor [ReCl$(CO)_3$(bpyC≡CH)].[8a] There is also some disorder involving the sites for the mutually-*trans* chloride and carbonyl ligands, which prevent further discussion. While the Au-S distances in **21** are very similar to those found in the structure of [Au($SC_6H_4CO_2H$-

4)(PPh_3)],[12a] the Au-P distance in the monometallic compound is a little longer [2.276(1) Å] compared to the value of 2.255(2) Å found for **21**. However, the deviation from linearity of the P-Au-S linkage in **21** [176.39(6)°] is much less than that found in the literature structure, of 168.95(4)°. This is likely to be due to the presence of short aurophilic contacts [Au…Au: 3.0756(2) Å] in the structure of [Au($SC_6H_4CO_2H$-4)(PPh_3)], which, along with probable packing effects, lead to distortion of this angle. No such interactions between gold(I) centres is observed in the structure of **21**. The ruthenium centre shows a distorted octahedtral geometry with cis-interlogand angles in the range 59.2(2) - 107.8(2)° with the smaller of these values correspondoing to the bite angle of the carboxylate chelate. This is close to the value for the same feature in the enynyl carboxylate complex [Ru(C(C≡CPh)=CHPh)($O_2CC_5H_4N$)(CO)(PPh_3)$_2$].[7d] In common with this compound, the structure of **21** displays differing ruthenium-oxygen bond lengths, with the Ru(1)-O(3) bond *trans* to the vinyl ligand being longer [2.233(4) Å] than the Ru(1)-O(1) bond distance [2.191(4) Å] *trans* to the carbonyl, indicating the superior *trans* influence of the former ligand over the latter. Overall, the structure of **21** does not appear to be overly congested from a steric viewpoint, though it is worth noting that both the $C_6H_4SAuPPh_3$ unit and the (bpy)ReCl$(CO)_3$ vinyl substituent are twisted with respect to the plane containing the carboxylate, vinyl and carbonyl ligands, the dihedral angles across the C2–C4 and C31–C34 bonds being 19.7(4) and 29.2(7)° respectively.

Synthesis of functionalized nanoparticles

Disulfides often require some persuasion (heat, extended reaction times) to react with low valent transition metals in molecular systems.[20] However, they are known to react readily with gold surfaces, whether two-dimensional SAMs[21] or gold nanoparticles,[22] driven by the formation of the favorable Au-S interaction. Throughout the reactions with metals described above, the disulfide linkage remained intact apart from when specifically targeted with a strong reducing agent. This protection represents a significant advantage in the design of nanoparticles functionalized with metal units, as the presence of a free thiol for attachment to the gold surface poses the risk of reacting instead with the metal center.[23] Strategies to overcome this include the initial attachment of the bifuntional tether to the metal nanoparticle through the thiol moiety followed by addition of molecular metal units to the terminal donor.[24] However, the relatively low reactivity of the disulfide moiety allows the construction of the metal unit before the RS-SR bond is activated by the presence of the gold surface.

With this in mind, compound **2** was used to add ruthenium units to the surface of gold nanoparticles using two common methods. Reduction of $HAuCl_4$ with sodium borohydride using the conditions popularized by Brust and Schiffrin[25] followed by addition of a methanol solution of **2** (Scheme 4) led to black nanoparticles, $Au^{2.9}$@[$SC_6H_4CO_2Ru(dppm)_2$]PF_6 (**NP1**), of average diameter 2.9 nm (± 0.2 nm), as determined by Transmission Electron Microscopy (TEM, see Supporting Information) (Figure 2a). The complete removal of unattached surface units was ensured through washing with dichloromethane and water. Infrared spectroscopy revealed the presence of the carboxylate unit ($\nu_{C\text{-}O}$ at 1575 cm^{-1}) as well as typical absorptions for the dppm units and a ν_{PF} absorption (817 cm^{-1}) indicating the continued presence of hexafluorophosphate counteranions. The material also proved sufficiently soluble in deuterated dimethylsulfoxide to record the ^1H NMR spectrum, which showed resonances for the PCH_2P protons at substantially shifted values of 4.44 and 5.76 ppm (compared to 3.88 and 5.05 ppm for **2** in dmso-d_6). As in the molecular complexes, the C_6H_4 resonances were obscured by the features associated with the phenyl groups of the dppm ligands between 6.89 and 7.74 ppm. The $^{31}P\{^1H\}$ NMR spectrum showed resonances at −18.6 and 3.2 ppm (J_{PP} = 35.7 Hz), which differ from the chemical shift values recorded for the precursor **2** (−12.7 and 9.3 ppm, J_{PP} = 39.1 Hz in dmso-d_6). This suggests a substantially different local environment for the ruthenium units when attached to the surface. The presence of gold and ruthenium was confirmed by Energy Dispersive X-ray Spectroscopy (EDS) measurements (Supporting Information), which also indicated the presence of sulfur, phosphorus, oxygen and fluorine (though this technique is less reliable for lighter elements). Thermogravimetric analysis (TGA) of a sample of **NP1** revealed the loss of 42.5% of the mass on gradual heating to 800 °C (Supporting Information). This can be assumed to be due to loss of the lighter elements and allows an approximate estimation of the number of surface units to be made. This loss of mass suggests a ratio of approximately 8.4:1 between the gold and [$SC_6H_4CO_2Ru(dppm)_2$]PF_6 surface units. Inductively-Coupled Plasma Atomic Emission Spectroscopy (ICP-AES) was also investigated to probe the number of surface units but complete dissolution of the samples in the recommended concentration of aqua regia proved difficult and so led to unreliable results. It has been noted that effective measurement of ruthenium by this method requires high temperature fusion with NaOH-$NaNO_3$ mixtures.[26]

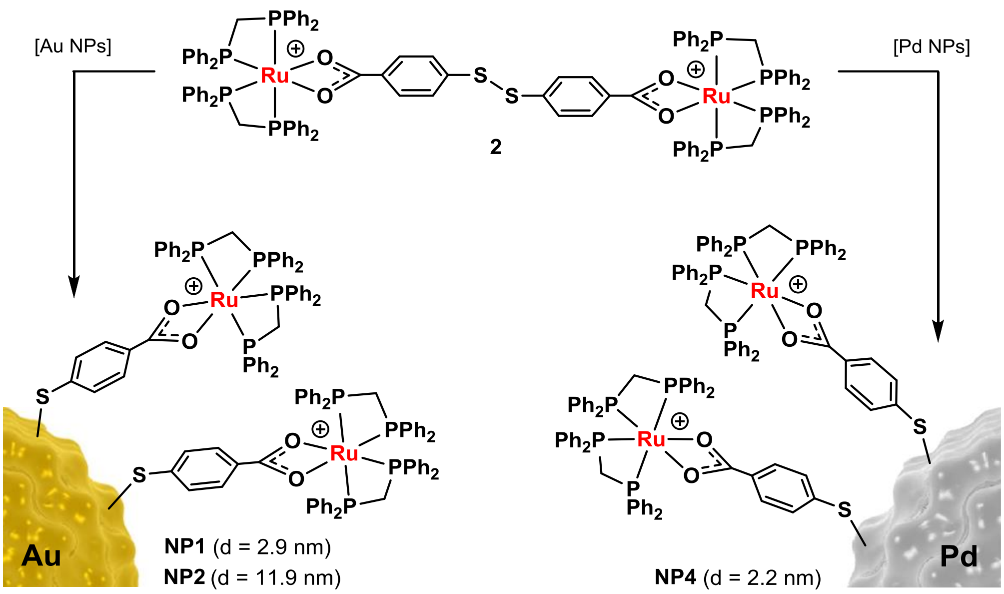

Scheme 4. Synthesis of functionalized gold and palladium nanoparticles bearing ruthenium surface units. All metal cations have hexafluorophosphate counteranions.

The citrate route, devised originally by Turkevich,[27] was also used to access black nanoparticles of larger average size. The resultant nanoparticles were found to possess a diameter of 11.9 nm (± 0.9 nm), as shown in TEM images (Figure 2b and 2c). As with **NP1**, EDS data indicated the presence of gold and ruthenium. Again, $^{31}P\{^1H\}$ and ^1H NMR spectroscopic data were recorded and were found to be consistent with the formulation $Au^{11.9}$@$[SC_6H_4CO_2Ru(dppm)_2]PF_6$ (**NP2**). The chemical shift values observed in the NMR spectra were very similar to those recorded for **NP1**, indicating a similarly dramatic change in environment compared to the molecular precursor **2**. The stapling effect in gold nanoparticles, whereby a gold atom is lifted from the surface and pinned between two thiolate units, is well established and has been observed crystallographically[28] and modelled computationally.[29] Potentially this is a route to loss of surface units through elimination of a gold(I) dithiolate unit, $Au(SR)_2^-$. In order to establish whether this was the case with these materials, the dichloromethane washings were analyzed but were found to contain only traces of unreacted $[\{Ru(dppm)_2(O_2CC_6H_4S\text{-}4)\}_2](PF_6)_2$ (**2**). The corresponding dithiolate $[Au\{SC_6H_4CO_2Ru(dppm)_2\}_2]PF_6$ (**10**) was not found to be present. Compound **10** contains only one hexafluorophosphate anion, whereas **2** posseses two of these counteranions, allowing them to be differentiated from the dppm : PF_6^- ratio provided by integration of their $^{31}P\{^1H\}$ NMR resonances. TGA data revealed a metallic residue of 57.5% of the original mass and so the remainder (42.5%) was ascribed to the mass of the surface units (excluding ruthenium). This equates to a stoichiometry of approximately $Au_{6.8}(SC_6H_4CO_2Ru(dppm)_2)PF_6$.

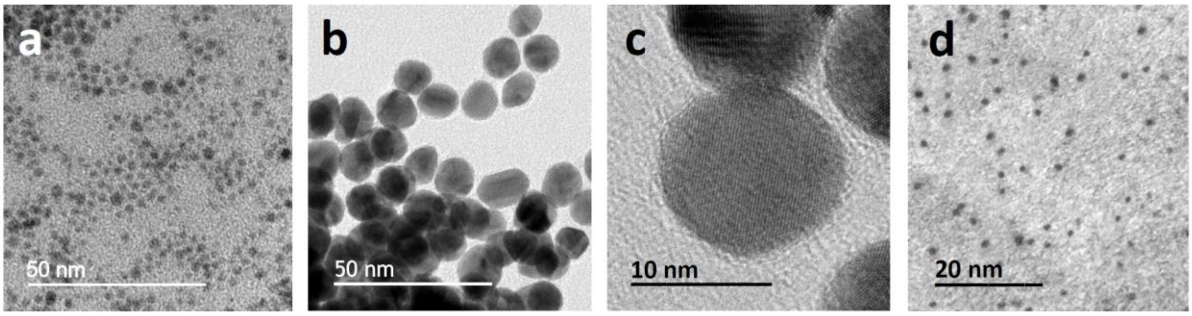

Figure 2. TEM images of a) **NP1**, b) **NP2**, c) **NP2** detail and d) **NP4**.

Ligand-stabilized gold nanoparticles can also be obtained through the reduction of well-defined gold(I) precursors containing phosphine,[30] amine,[31] alkyl,[32] carboxylate[33] and carbene[34] ligands. Given their ready thermal reduction in the gilding process of ceramics,[35] it is not surprising that gold(I) thiolate precursors (often polymeric or cyclic species) have also been employed in the direct preparation of thiolate-capped gold nanoparticles.[36a-c] This approach has been further developed using e-beam lithography/thermolysis protocols.[36d,e] Thermolysis of monometallic gold(I) dithiolate complexes has been used to generate gold nanoparticles stabilized by alkyl groups,[37] while molecular methylgold(I) precursors have been employed in the presence of thiol surfactants to prepare thiolate-protected gold nanoparticles by a thermal route (140 °C).[32] We have recently reported[29e] that the metallacylic digold complexes $[Au_2(S_2CNR_2)_2]$ ($NR_2 = N(CH_2CH{=}CH_2)_2$, NC_4H_6) undergo reduction to form gold nanoparticles with diameters 4.0 or 4.8 nm (± 0.7 nm). The presence of intramolecular and intermolecular aurophilic interactions (probed by structural investigations)[38] in these complexes offers a fascinating suggestion[31b] as to the role these interactions (15-30 KJ mol^{-1} and so comparable in strength to hydrogen bonding) might play in facilitating the formation of nanoparticles from such complexes. Accordingly, it was decided to explore whether direct preparation of nanoparticles from $[Au\{SC_6H_4CO_2Ru(dppm)_2\}_2]PF_6$ (**10**) was possible either thermally or by using sodium borohydride as the reducing agent. However, these attempts failed to yield nanoparticles. This showed that **10** was sufficiently robust to withstand heating at reflux (in acetone, 1,2-dichloroethane) or the addition of a large excess of reducing agent. In contrast, treating a solution of the monometallic precursor, PPN[$Au(SC_6H_4CO_2H\text{-}4)_2$] (PPN = bis(triphenylphosphine)iminium) in acetone with excess sodium borohydride results in the darkening of the solution and the formation of a black solid, formulated as $Au@SC_6H_4CO_2H$-4 (**NP3**). This surface unit was also used in the $Au_{102}(SC_6H_4CO_2H\text{-}4)_{44}$ nanoparticles structurally determined by X-ray diffraction reported by Kornberg and co-workers.[28a] Analysis by TEM (Supporting Information) revealed the formation of nanoparticles with a relatively wide size distribution (4.1 ± 0.7 nm), while the solid state infrared spectrum displays absorptions typical of 4-mercaptobenzoic acid ($\nu_{C\text{-}O}$ at 1587 cm^{-1}). It was thought that the explanation for the difference in the propensity of PPN[$Au(SC_6H_4CO_2H\text{-}4)_2$] and **10** to form nanoparticles could be related to the presence or absence of aurophilic interactions. Compound **10** bears two bulky $Ru(dppm)_2$ units in reasonably close proximity to the gold(I) center, while the precursor has a much smaller steric profile and could indeed permit aurophilic interactions. The structure of this compound has not been reported but structural data for some related dithiolate compounds have been determined. From these reports, it appears that the nature of the countercation exerts considerable influence on whether short intramolecular gold-gold contacts are observed. The structure of $\{K_3[Au(mba)_2]\}_2$ (H_2mba = 2-mercaptobenzoic acid)[39a] displays a short separation between dimeric units (3.1555(7) Å) but no additional interactions between neighboring dimers, while the structures of [$^nBu_4N$][$Au(SC_6H_4\text{-}R)_2$] (R = *ortho*-Me, *ortho*-Cl, *meta*-Cl) show no aurophilic contacts, an observation which is attributed to the bulky nature of the countercation.[39b]

In order to broaden the study beyond attachment to gold surfaces, the generation and functionalization of palladium nanoparticles with **2** was investigated. The divalent palladium precursor [$PdCl_2(NCMe)_2$] was reduced by lithium triethylborohydride in the presence of the phase transfer agent, tetraoctylammonium bromide (TOAB)[40] before addition of a solution of compound **2**. After washing the resultant black nanoparticles to remove TOAB and unreacted **2**, the material Pd@[$SC_6H_4CO_2Ru(dppm)_2$]PF_6 (**NP4**) was isolated. This proved insoluble in all common deuterated solvents, preventing NMR analysis, however, infrared spectroscopy revealed typical features for the surface units as observed for **NP1** and **NP2**. TEM images showed typically small[24b] nanoparticles of only 2.2 nm (± 0.2 nm) diameter (Figure 1d), while EDS analysis indicated the presence of palladium and ruthenium as well as the expected lighter elements. A metallic residue of 61.6% (palladium and ruthenium) was observed from TGA investigations with the remaining 38.4% of the mass attributed to the rest of the elements in the surface units. This suggested that the ratio of palladium to surface units is close to 15:1, indicating a sparsely covered nanoparticle surface.

Conclusions

In the systems described here, the significantly lower reactivity of the disulfide linkage (compared to that of the carboxylate donors) prevents unwanted reaction of the sulfur moiety until intended. This allows chelation by the oxygen donors to dominate initial coordination of the transition metals employed, while allowing subsequent activation of the disulfide through reduction or addition to a nanoparticle surface. This strategy is illustrated by the preparation of a series of heterobimetallic Ru-Au complexes. An alternative route to the same compounds is provided by the reaction of 4-mercaptobenzoic acid with thiophilic gold(I) precursors followed by activation (addition of base) and coordination of the oxygen donors to ruthenium or osmium. This also allows the preparation of pentametallic complexes containing Fe, Ru and Au. Exploitation of the two centers of reactivity possessed by ruthenium and osmium vinyl complexes (i.e. the metal center and the vinyl substituent), allows heterotrimetallic ReOsAu, heterotetrametallic Re_2Os_2 and heteroheptametallic $Re_2FeOs_2Au_2$ assemblies to be prepared in a controlled, stepwise manner. Furthermore, the same diruthenium disulfide complex (**2**) used as the starting point in the above studies, serves as an easily prepared and versatile precursor for the surface functionalization of gold and palladium nanoparticles. This versatility allows the same design approach to be applied to the assembly of both molecular and nanoscale multimetallic assemblies.

Experimental Section

General Comments. Unless otherwise stated, all experiments were carried out in air and the complexes obtained appear stable towards the atmosphere, whether in solution or in the solid state. Reagents and solvents were used as received from commercial sources. Petroleum ether is the fraction boiling in the 40–60 °C range. The following complexes were prepared as described elsewhere: $[AuCl(PR_3)]$ (R = Me,[41] Cy,[42] Ph[43]), $[dppf(AuCl)_2]$,[44] [AuCl(IDip)],[45] $[Au(SC_6H_4CO_2H\text{-}4)_2]PPN$,[12] *cis*-$[RuCl_2(dppm)_2]$,[46] $[M(CH{=}CHC_6H_4Me\text{-}4)Cl(CO)(BTD)(PPh_3)_2]$ (M = Ru,[14,17b] Os[15]), $[Ru(C(C{\equiv}CPh){=}CHPh)(CO)(PPh_3)_2]$[47] and

$[Os\{CH=CH\text{-}bpyReCl(CO)_3\}Cl(CO)(BTD)(PPh_3)_2]$.[7a] All glassware used for nanoparticle preparation was washed with aqua regia and rinsed thoroughly with ultrapure water before use. Electrospray (ES) and Fast Atom Bombardment (FAB) mass data were obtained using Micromass LCT Premier and Autospec Q instruments, respectively. Infrared data were obtained using a Perkin-Elmer Spectrum 100 FT-IR spectrometer and characteristic triphenylphosphine-associated infrared data are not reported. NMR spectroscopy was performed at 25 °C using Varian Mercury 300, Bruker AV400 and Bruker 500 Avance III HD spectrometers in $CDCl_3$ unless stated otherwise. All coupling constants are in Hertz. Resonances in the $^{31}P\{^1H\}$ NMR spectrum due to the hexafluorophosphate counteranion were observed where the formulation indicates but are not included below. Elemental analysis data were obtained from London Metropolitan University. Solvates were confirmed by integration of the ^1H NMR spectra. The procedures given provide materials of sufficient purity for synthetic and spectroscopic purposes. TEM images and EDS data were obtained at Imperial College using a JEOL 2010 high-resolution TEM (80-200 kV) equipped with an Oxford Instruments INCA EDS 80mm X-Max detector system. Thermogravimetric analysis was performed on a Mettler Toledo DSC 1LF/UMX Thermogravimetric Analyzer, using a platinum sample holder. ICP-AES analyses were performed using a Perkin-Elmer 2000 DV ICP-OE spectrometer.

$(SC_6H_4CO_2H\text{-}4)_2$ (1)

A solution of iodine (1M in MeOH) was added dropwise to a colorless solution of 4-mercaptobenzoic acid (450 mg, 2.92 mmol) in MeOH (60 mL) until the mixture took on a persistent orange coloration. The cloudy mixture was stirred for a further 30 minutes and then filtered. The resulting white solid was washed several times with ethanol and dried under vacuum overnight. Yield: 400 mg (90%). IR (solid state): 2838, 2669, 2552, 1676 ($\nu_{C\text{-}O}$), 1591, 1423, 1323, 1292, 1181, 1116, 933, 850 cm^{-1}; ^1H NMR (dmso-d_6): δ 7.52, 7.81 (d x 2, J_{HH} = 8.0 Hz, 2 x 4 H; C_6H_4) ppm. The CO_2H protons were not observed. These data agree well with literature values.[10]

$[\{Ru(dppm)_2(O_2CC_6H_4S\text{-}4)\}_2](PF_6)_2$ (2)

A solution of *cis*-$[RuCl_2(dppm)_2]$ (263 mg, 0.280 mmol) in dichloromethane (50 mL) was treated with a solution of **1** (43.0 mg, 0.140 mmol), sodium methoxide (30.0 mg, 0.555 mmol), and ammonium hexafluorophosphate (91.0 mg, 0.558 mmol) in methanol (25 mL).

The reaction mixture was stirred for 2 h at room temperature. All solvent was removed under vacuum and the crude product was dissolved in dichloromethane (10 mL) and filtered through Celite to remove NaCl, NaOMe, and excess ligand. Ethanol (20 mL) was added and the solvent volume was slowly reduced on a rotary evaporator until the precipitation of the yellow solid was complete. This was filtered, washed with petroleum ether (10 mL), and dried under vacuum. Yield: 281 mg (86%). IR (solid state): 3058, 1590 ($\nu_{C\text{-}O}$), 1484, 1426, 1189, 1097, 834 (ν_{PF}) cm^{-1}; ^{1}H NMR (dichloromethane–d$_2$): δ 3.95, 4.63 (m x 2, 2 x 4H; PCH_2P), 6.18 (m, 8H; C_6H_5), 6.92 − 7.76 (m, 72H + 8H; C_6H_5 + C_6H_4) ppm; ^{31}P{^{1}H} NMR (dmso–d$_6$): δ −12.0, 8.9 (pseudotriplet x 2, J_{PP} = 39.0 Hz; dppm) ppm; ^{1}H NMR (dmso–d$_6$): δ 3.88, 5.05 (m x 2, 2 x 4H; PCH_2P), 6.14 (m, 8H; C_6H_5), 6.86 − 7.77 (m, 72H + 8H; C_6H_5 + C_6H_4) ppm; ^{13}C{^{1}H} NMR (CD_2Cl_2, 500 MHz): δ = 181.7 (s, CO_2), 141.9 (s, CS), 134.9 (s, CCO_2), 133.8, 132.4, 132.1 (m x 3, C_6H_5), 131.7 (s, *o/m*-C_6H_4), 131.3 (m, C_6H_5), 131.1, 130.8 (s x 2, C_6H_5), 130.4 (s, *o/m*-C_6H_4), 129.6, 129.4, 129.3, 128.8 (m x 4, C_6H_5), 126.4, 126.2 (s x 2, C_6H_5), 43.6 (t, J_{PC} = 11.5 Hz, PCH_2P) ppm. ^{31}P{^{1}H} NMR (dmso–d$_6$): δ −12.7, 9.3 (pseudotriplet x 2, J_{PP} = 39.1 Hz; dppm) ppm; MS (FAB +ve) *m/z* (%) 2044 (5) $[M]^+$; Anal. Calcd (%) for $C_{114}H_{96}F_{12}O_4P_{10}Ru_2S_2$ (M_w = 2333.97): C 58.7, H 4.2 %. Found: C 58.6, H 4.2 %.

$[Ru(dppm)_2(O_2CC_6H_4SH\text{-}4)]PF_6$ (3)

Solid sodium borohydride (8.0 mg, 0.21 mmol) was added at 0 °C to a solution of **2** (115 mg, 0.049 mmol) in dichloromethane (15 mL). After stirring for 4 h, the solution was adjusted to pH 4 through addition of 4M HCl solution. The organic layer was then washed with water (20 mL), brine (20 mL) and dried over Na_2SO_4. All solvent was removed under vacuum and the resulting yellow powder was washed with diethyl ether (10 mL). This was dried under vacuum. Yield: 73 mg (64%). IR (solid state): 3056, 1595 ($\nu_{C\text{-}O}$), 1484, 1428, 1095, 1000, 830 (ν_{PF}) cm^{-1}. ^{1}H NMR: δ 4.06, 4.72 (m x 2, 2 x 2H; PCH_2P), 6.10 – 6.18 (m, 4H; C_6H_5), 6.99 − 7.77 (m, 36H + 4H; C_6H_5 + C_6H_4) ppm; ^{31}P{^{1}H} NMR: δ −11.9, 8.8 (pseudotriplet x 2, J_{PP} = 39.0 Hz; dppm) ppm; MS (ES +ve) *m/z* (%) 1024 (50) $[M + H]^+$; Anal. Calcd (%) for $C_{57}H_{49}F_6O_2P_5RuS\cdot 4CH_2Cl_2$ (M_w = 1507.72, M_w = 1167.99 in absence of solvation): C 48.6, H 3.8 %. Found: C 48.5, H 4.0 %.

[(dppm)$_2$Ru(O$_2$CC$_6$H$_4$S-4)Au(PPh$_3$)]PF$_6$ (4)

A solution of [Au(SC$_6$H$_4$CO$_2$H-4)(PPh$_3$)] (19 mg, 0.031 mmol), sodium methoxide (2.7 mg, 0.050 mmol) and ammonium hexafluorophosphate (5.0 mg, 0.031 mmol) in dichloromethane (5 mL) and methanol (2 mL) was added dropwise to a stirred solution of *cis*–[RuCl$_2$(dppm)$_2$] (28 mg, 0.030 mmol) in dichloromethane (10 mL). After stirring for 4 h, all solvent was removed under vacuum. The residue was dissolved in dichloromethane (10 mL) and filtered through celite to remove inorganic salts. The solvent was removed and the resulting yellow powder was washed with diethyl ether (10 mL). This was dried under vacuum. Yield: 38 mg (75%). IR (solid state): 3055, 1587 ($\nu_{C\text{-}O}$), 1481, 1435, 1419, 1175, 1098, 833 (ν_{PF}), 730, 690 cm^{-1}. ^{1}H NMR (dichloromethane–d$_2$): δ 3.90, 4.62 (m x 2, 2 x 2H; PCH$_2$P), 6.15 – 6.20 (m, 4H; C$_6$H$_5$), 6.99 – 7.80 (m, 51H + 4H; C$_6$H$_5$ + C$_6$H$_4$) ppm. ^{13}C{^{1}H} NMR (CD$_2$Cl$_2$, 500 MHz): δ = 183.4 (s, CO$_2$), 151.3 (s, CS), 134.5 (d, J_{PC} = 11.0 Hz, *o/m*-AuPC$_6$H$_5$), 133.9 (m, RuPC$_6$H$_5$), 133.7 (s, CCO$_2$), 132.4 (m, RuPC$_6$H$_5$), 132.3 (s, RuPC$_6$H$_5$), 132.1 (s, *o/m*-C$_6$H$_4$), 131.6 (s, *p*-AuPC$_6$H$_5$), 131.3, 130.9 (m x 2, RuPC$_6$H$_5$), 130.7 (s, RuPC$_6$H$_5$), 130.4 (s, *o/m*-C$_6$H$_4$), 129.7 (m, *o/m*-AuPC$_6$H$_5$ + *ipso*-AuPC$_6$H$_5$), 129.6, 129.4, 128.9, 128.7 (m x 4, RuPC$_6$H$_5$), 128.2 (s, RuPC$_6$H$_5$), 43.6 (t, J_{PC} = 13.0 Hz, PCH$_2$P) ppm. ^{31}P{^{1}H} NMR (dichloromethane–d$_2$): δ −12.1, 8.9 (pseudotriplet x 2, J_{PP} = 39.0 Hz; dppm), 38.5 (s; PPh$_3$) ppm. MS (ES +ve) *m/z* (%) 1481 (60) [M]$^+$; Anal. Calcd (%) for C$_{75}$H$_{63}$AuF$_6$O$_2$P$_6$RuS (M$_w$ = 1626.24): C 55.4, H 3.9 %. Found: C 55.5, H 3.7 %.

[Au(SC$_6$H$_4$CO$_2$H-4)(PCy$_3$)] (5)

A solution of 4–mercaptobenzoic acid (15 mg, 0.097 mmol) and sodium methoxide (6.0 mg, 0.11 mmol) in methanol (5 mL) was added dropwise to a stirred solution of [AuCl(PCy$_3$)] (50 mg, 0.098 mmol) in dichloromethane (10 mL). After stirring for 2 h, all solvent was removed under vacuum. The residue was dissolved in dichloromethane (10 mL) and filtered through celite to remove NaCl. Pentane (25 mL) was then added resulting in the precipitation of a colorless solid. This was filtered and dried under vacuum. Yield: 36 mg (58%). IR (solid state): 2920, 2852, 1446, 1348, 1293, 1265, 1174, 1113, 1004, 888, 850, 739 cm^{-1}. ^{1}H NMR (acetone–d$_6$): δ 1.30 – 2.84 (m, 33H; PCy$_3$), 7.56, 7.70 (d x 2, J_{HH} = 8.6 Hz, 4H; C$_6$H$_4$). ^{31}P{^{1}H} NMR (acetone–d$_6$): δ 58.3 (s; PCy$_3$) ppm. MS (ES +ve) m/z (%) 981 (60) [2M – PCy$_3$]$^+$; Anal. Calcd (%) Calculated for Calculated for C$_{25}$H$_{38}$AuO$_2$PS·CH$_2$Cl$_2$ (M$_w$ = 715.51, M$_w$ = 630.57 in absence of solvation): C 43.6, H 5.6 %. Found: C 43.1, H 5.6 %.

[(dppm)$_2$Ru(O$_2$CC$_6$H$_4$S-4)Au(PCy$_3$)]PF$_6$ (6)

Using the same procedure employed in the preparation of **4**, with [Au(SC$_6$H$_4$CO$_2$H-4)(PCy$_3$)] (22 mg, 0.035 mmol), sodium methoxide (2.0 mg, 0.037 mmol), ammonium hexafluorophosphate (5.5 mg, 0.034 mmol) and *cis*-[RuCl$_2$(dppm)$_2$] (32 mg, 0.034 mmol) provided a yellow solid. Yield: 29 mg (52 %). IR (solid state): 3057, 2925, 2852, 1706, 1586 ($\nu_{C\text{-}O}$), 1482, 1418, 1261, 1094, 834 (ν_{PF}), 729, 691 cm^{-1}. ^{1}H NMR (CD$_2$Cl$_2$): δ 1.30 – 2.16 (m, 33H; PCy$_3$), 3.90, 4.63 (m x 2, 2 x 2H; PCH$_2$P), 6.18 (m, 4H; C$_6$H$_5$), 6.96 – 7.99 (m, 36H + 4H; C$_6$H$_5$ + C$_6$H$_4$) ppm. ^{31}P{^{1}H} NMR (dichloromethane–d$_2$): δ −12.1, 8.9 (pseudotriplet x 2, J_{PP} = 39.0 Hz; dppm), 57.6 (s; PPh$_3$) ppm. MS (ES +ve) *m/z* (%) 1500 (100) [M]$^+$; Anal. Calcd (%) for C$_{75}$H$_{81}$AuF$_6$O$_2$P$_6$RuS (M$_w$ = 1644.38): C 54.8, H 5.0 %. Found C 54.4, H 5.2 %.

[(dppm)$_2$Ru(O$_2$CC$_6$H$_4$S-4)Au(PMe$_3$)]PF$_6$ (7)

Employing the same procedure used to prepare **4**, reaction between [Au(SC$_6$H$_4$CO$_2$H-4)(PMe$_3$)] (21 mg, 0.049 mmol), sodium methoxide (3.0 mg, 0.056 mmol), ammonium hexafluorophosphate (8.0 mg, 0.049 mmol) and *cis*–[RuCl$_2$(dppm)$_2$] (46 mg, 0.049 mmol) provided a yellow solid. Yield: 44 mg (62%). IR (solid state): 3056, 1916, 1586 ($\nu_{C\text{-}O}$), 1481, 1482, 1419, 1262, 1174, 1094, 960, 832 (ν_{PF}), 729, 690 cm^{-1}. ^{1}H NMR (acetone–d$_6$): δ 1.75 (d, J_{HP} = 11.0 Hz, 9H; PMe$_3$), 4.12, 5.02 (m x 2, 2 x 2H; PCH$_2$P), 6.34 (m, 4H; C$_6$H$_5$), 7.04 – 8.00 (m, 36H + 4H; C$_6$H$_5$ + C$_6$H$_4$) ppm. ^{31}P{^{1}H} NMR (acetone–d$_6$): δ −12.8, 8.9 (pseudotriplet x 2, J_{PP} = 39 Hz; dppm), 0.6 (s; PMe$_3$) ppm. MS (ES +ve) *m/z* (%) 1295 (100) [M]$^+$; Anal. Calcd (%) for C$_{60}$H$_{57}$AuF$_6$O$_2$P$_6$RuS (M$_w$ = 1440.03): C 50.0, H 4.0 %. Found: C 49.9, H 4.1 %.

[Au(SC$_6$H$_4$CO$_2$H-4)(IDip)] (8)

Using the same procedure as employed for **5**, reaction of 4–mercaptobenzoic acid (12 mg, 0.078 mmol), sodium methoxide (4.5 mg, 0.083 mmol) and [AuCl(IDip)] (50 mg, 0.081 mmol) provided a colorless solid. Yield: 50 mg (84%). IR (solid state): 2961, 1671, 1581 ($\nu_{C\text{-}O}$), 1415, 1281, 1171, 1084, 936, 801, 755 cm^{-1}. ^{1}H NMR (acetone–d$_6$): δ 1.28 (d, J_{HH} = 6.9 Hz, 12H; CH$_3$), 1.37 (d, J_{HH} = 6.9 Hz, 12H; CH$_3$), 2.74 (sep, J_{HH} = 6.9 Hz, 4H; *CH*Me$_2$), 6.84, 7.42 (d x 2, J_{HH} = 8.2 Hz, 4H; C$_6$H$_4$), 7.48 (d, J_{HH} = 7.8 Hz, 4H; *m*–C$_6$H$_3$), 7.64 (t, J_{HH} = 7.8 Hz, 2H; *p*–C$_6$H$_3$), 7.87 (s, 2H; NCH) ppm. MS (ES +ve) *m/z* (%): 739 (10) [M]$^+$. Anal.

Calcd (%) for $C_{34}H_{41}AuN_2O_2S$ (M_w = 738.73): C 55.3, H 5.6, N 3.8 %. Found: C 55.2, H 5.7, N 3.9 %.

[(dppm)$_2$Ru(O$_2$CC$_6$H$_4$S-4)Au(IDip)]PF$_6$ (9)

Using the same procedure as employed for **4**, reaction of **8** (18 mg, 0.024 mmol), sodium methoxide (1.4 mg, 0.026 mmol), ammonium hexafluorophosphate (4.1 mg, 0.025 mmol) and *cis*–[RuCl$_2$(dppm)$_2$] (24 mg, 0.026 mmol) provided a yellow solid. Yield: 28 mg (62%). IR (solid state): 2960, 1585 ($\nu_{C\text{-}O}$), 1471, 1416, 1174, 1093, 837 (ν_{PF}), 734, 692 cm^{-1}. ^{1}H NMR (dichloromethane–d$_2$): δ 1.25, 1.33, 1.39, 1.44 (d x 4, J_{HH} = 6.9 Hz, 4 x 6H; Me), 2.77 (sep, J_{HH} = 6.9 Hz, 4H; *CH*Me$_2$), 3.89, 4.63 (m x 2, 2 x 2 H; PCH$_2$P), 6.34 (m, 4H; C$_6$H$_5$), 6.83 (d, J_{HH} = 8.1 Hz, 2H; C$_6$H$_4$), 7.06 – 7.55 (m, 28H + 2H + 4H; C$_6$H$_5$ + C$_6$H$_4$ + *m*-C$_6$H$_3$), 7.64 (t, J_{HH} = 7.8 Hz, 2H; *p*-C$_6$H$_3$), 7.83 (m, 4H; C$_6$H$_5$), 7.91 (s, 2H; NCH), 8.01 (m, 4H; C$_6$H$_5$) ppm. ^{31}P{^{1}H} NMR (acetone–d$_6$): δ −12.9, 9.0 (pseudotriplet x 2, J_{PP} = 39.0 Hz; dppm) ppm. MS (ES +ve) *m/z* (%) 1607 (100) [M]$^+$; Anal. Calcd (%) for $C_{84}H_{84}AuF_6N_2O_2P_5RuS$ (M_w = 1752.54): C 57.6, H 4.8, N 1.6 %. Found: C 57.4, H 4.8, N 1.6 %.

[Au{SC$_6$H$_4$CO$_2$Ru(dppm)$_2$}$_2$]PF$_6$ (10)

A solution of *cis*–[RuCl$_2$(dppm)$_2$] (55 mg, 0.059 mmol) in dichloromethane (10 mL) was added to [N(PPh$_3$)$_2$][Au(SC$_6$H$_2$CO$_2$H)$_2$] (30 mg, 0.029 mmol), ammonium hexafluorophosphate (19 mg, 0.12 mmol) and sodium methoxide (6.0 mg, 0.111 mmol) in mixture of methanol (5 mL) and dichloromethane (2 mL). The reaction mixture was stirred for 2 h at room temperature. All solvent was removed under vacuum and the crude product was dissolved in dichloromethane (10 mL) and filtered through Celite to remove NaCl, NaOMe, and excess ligand. Ethanol (20 mL) was added and the solvent volume was slowly reduced on a rotary evaporator until the precipitation of the yellow product was complete. This was filtered, washed with cold ethanol (5 mL) petroleum ether (10 mL), and dried under vacuum. Yield: 49 mg (71%). IR (solid state): 1590 ($\nu_{C\text{-}O}$), 1484, 1426, 1312, 1261, 1177, 1094, 1027, 1014, 1000, 834 (ν_{PF}) cm^{-1}; ^{1}H NMR (DMSO–d$_6$): δ 3.88 (m, 2 x 2H; PCH$_2$P), 5.01 (m, 2 x 2H; PCH$_2$P), 6.12 (m, 8H; C$_6$H$_5$), 6.86 − 7.75 (m, 72H + 8H; C$_6$H$_5$ + C$_6$H$_4$) ppm. ^{31}P{^{1}H} NMR (DMSO–d$_6$): δ −7.94 (pseudotriplet, J_{PP} = 39.0 Hz; dppm), 14.02 (pseudotriplet, J_{PP} = 39.0 Hz; dppm) ppm; MS (ES +ve) *m/z* (%) 2044 (100) [M – Au]$^+$;

Anal. Calcd (%) for $C_{114}H_{96}AuF_6O_4P_9Ru_2S_2$ (M_w = 2385.97): C 57.4, H 4.1 %. Found: C 57.2, H 4.0 %.

[(dppf){AuSC$_6$H$_4$CO$_2$Ru(dppm)$_2$}$_2$](PF$_6$)$_2$ (11)

A solution of [dppf(AuSC$_6$H$_4$CO$_2$H-4)$_2$] (12 mg, 0.010 mmol), sodium methoxide (1.0 mg, 0.019 mmol) and ammonium hexafluorophosphate (4.9 mg, 0.030 mmol) in dichloromethane (5 mL) and methanol (2 mL) was added dropwise to a stirred solution of *cis*–[RuCl$_2$(dppm)$_2$] (18.8 mg, 0.020 mmol) in dichloromethane (10 mL). After stirring for 4 h, all solvent was removed under vacuum. The residue was filtered and washed with water (10 mL) and pentane (5 mL) providing a pale yellow powder. This was dried under vacuum. Yield: 20 mg (61%). IR (solid state): 1587 ($\nu_{C\text{-}O}$), 1483, 1435, 1173, 1099, 1027, 835 (ν_{PF}), 731, 692 cm^{-1}. ^{1}H NMR (acetone–d$_6$): δ 3.98 (m, 4 H; PCH$_2$P), 4.24, 4.63 (s x 2, 2 x 4H; C$_5$H$_4$), 4.95 (m, 4 H; PCH$_2$P), 6.21 (m, 4 H; C$_6$H$_5$), 6.49, 6.63 (m x 2, 2 x 2H; C$_6$H$_4$), 6.81 – 7.80 (m, 76 H + 8 H; C$_6$H$_5$ + C$_6$H$_4$) ppm; ^{31}P{^{1}H} NMR: δ −13.7, 7.5 (pseudotriplet x 2, J_{PP} = 39.0 Hz; dppm), 27.7 (s; dppf) ppm. MS (MALDI) *m/z* (%) 3031 (12) [M + K]$^+$. Anal. Calcd (%) for $C_{148}H_{124}Au_2F_{12}FeO_4P_{12}Ru_2S_2$ (M_w = 3282.24): C 54.2, H 3.8 %. Found: C 54.4, H 3.9 %.

[{Ru(CH=CHC$_6$H$_4$Me-4)(CO)(PPh$_3$)$_2$(O$_2$CC$_6$H$_4$S-4)}$_2$] (12)

Using the same procedure used to prepare **2**, reaction between compound **1** (6.4 mg, 0.021 mmol), sodium methoxide (2.3 mg, 0.043 mmol) and [Ru(CH=CHC$_6$H$_4$Me–4)Cl(CO)(BTD)(PPh$_3$)$_2$] (40 mg, 0.042 mmol) provided an orange solid. Yield: 24 mg (62%). IR (solid state): 1917 (ν_{CO}), 1575 ($\nu_{C\text{-}O}$), 1507, 1481, 1418, 1185, 1094, 862, 742, 691 cm^{-1}. ^{1}H NMR (CD$_2$Cl$_2$): δ 2.22 (s, 6H; CH$_3$), 5.85 (d, J_{HH} = 15.5 Hz, 2H; Hβ), 6.38, 6.82 (d x 2, J_{HH} = 7.8 Hz, 2 x 4H; C$_6$*H*$_4$Me), 7.05, 7.10 (d x 2, J_{HH} = 8.6 Hz, 2 x 4H; C$_6$H$_4$S), 7.28 – 7.51 (m, 60H; C$_6$H$_5$), 7.82 (dt, J_{HH} = 15.5 Hz, J_{HP} unresolved, 2H; Hα) ppm. ^{13}C{^{1}H} NMR (CD$_2$Cl$_2$, 400 MHz): δ 202.4 (t, J_{PC} = 11.3 Hz, CO), 176.4 (s, CO$_2$), 152.5 (s, CS), 139.2 (t(br), J_{PC} unresolved, Cα), 138.1 (s, C$^{1/4}$-C$_6$H$_4$), 134.3 (t^v, J_{PC} = 5.5 Hz; *o/m*-C$_6$H$_5$), 133.4 (t(br), J_{PC} unresolved, Cβ), 132.9, 132.0, 131.9 (s x 3, C$^{1/4}$-C$_6$H$_4$), 131.3 (t^v, J_{PC} = 21.3 Hz; *ipso*-C$_6$H$_5$), 129.8 (s, *p*-C$_6$H$_5$), 128.5, 128.2 (s x 2, *o/m*-C$_6$H$_4$), 127.9 (t^v, J_{PC} = 3.9 Hz, *o/m*-C$_6$H$_5$), 125.3, 124.5 (s x 2, *o/m*-C$_6$H$_4$), 20.6 (s, CH$_3$) ppm. ^{31}P{^{1}H} NMR (CD$_2$Cl$_2$): δ 37.7 (s; PPh$_3$) ppm. MS (ES +ve) *m/z* (%) 1885 (2) [M + K]$^+$, 1175 (14) [M – vinyl – CO – 2PPh$_3$]$^+$. Anal. Calcd (%) for $C_{106}H_{86}O_6P_4Ru_2S_2$ (M_w = 1845.98): C 69.0, H 4.7 %. Found: C 68.8, H 4.8 %.

[{Os(CH=CHC$_6$H$_4$Me-4)(CO)(PPh$_3$)$_2$(O$_2$CC$_6$H$_4$S-4)}$_2$] (13)

Using the same procedure employed to prepare **2**, reaction between compound **1** (5.8 mg, 0.019 mmol), sodium methoxide (2.0 mg, 0.037 mmol) and [Os(CH=CHC$_6$H$_4$Me–4)Cl(CO)(BTD)(PPh$_3$)$_2$] (40 mg, 0.039 mmol) provided a yellow solid. Yield: 26 mg (66%). IR (solid state): 1906 (ν_{CO}), 1592 ($\nu_{C\text{-}O}$), 1507, 1482, 1433, 1186, 1095, 868, 742, 691 cm^{-1}. ^{1}H NMR (acetone–d$_6$): δ 2.21 (s, 6H; CH$_3$), 5.78 (d, J_{HH} = 16.0 Hz, 2H; Hβ), 6.37, 6.75 (d x 2, J_{HH} = 7.8 Hz, 2 x 4H; C$_6$*H*$_4$Me), 7.08, 7.20 (d x 2, J_{HH} = 8.6 Hz, 2 x 4H; C$_6$H$_4$S), 7.32 – 7.48 (m, 60H; C$_6$H$_5$), 8.21 (dt, J_{HH} = 16.0, J_{HP} = 2.1 Hz, 2H; Hα) ppm. ^{31}P{^{1}H} NMR (acetone–d$_6$): δ 18.5 (s; PPh$_3$) ppm. MS (ES +ve) *m/z* (%) 2025 (46) [M]$^+$; Anal. Calcd (%) for C$_{106}$H$_{86}$O$_6$Os$_2$P$_4$S$_2$ (M$_w$ = 2024.30): C 62.9, H 4.3 %. Found: C 62.8, H 4.2 %.

[{Os{CH=CH-bpyReCl(CO)$_3$}(CO)(PPh$_3$)$_2$(O$_2$CC$_6$H$_4$S-4)}$_2$] (14)

Using the same procedure used to prepare **2**, reaction between compound **1** (5.5 mg, 0.018 mmol), sodium methoxide (2.0 mg, 0.037 mmol) and [Os{CH=CH–bpyReCl(CO)$_3$}Cl(CO)(BTD)(PPh$_3$)$_2$] (50 mg, 0.036 mmol) provided an orange solid. Yield: 44 mg (89%). Recrystallization from a dichloromethane solution of **13** layered with diethyl ether produced microcrystals, which were used for elemental analysis. IR (solid state): 2015 (ν_{CO}), 1882 (ν_{CO}), 1586 ($\nu_{C\text{-}O}$), 1433, 1352, 1184, 1094, 745, 692 cm^{-1}. ^{1}H NMR (acetone–d$_6$): δ 5.72 (d, J_{HH} = 16.2 Hz, 2H; Hβ), 7.14, 7.22 (d x 2, J_{HH} = 8.4 Hz, 2 x 4H; C$_6$H$_4$S), 7.30 – 7.46 (m, 60H + 2H; C$_6$H$_5$ + bpy), 7.65 (t, J_{HH} = 6.4 Hz, 2H; bpy), 8.00 (s, 2H; bpy), 8.14 (d, J_{HH} = 8.3 Hz, 2H; bpy), 8.22 (t, J_{HH} = 7.6 Hz, 2H; bpy), 8.41 (d, J_{HH} = 7.6 Hz, 2H; bpy), 9.01 (d, J_{HH} = 4.7 Hz, 2H; bpy), 9.36 (dt, J_{HH} = 16.2 Hz, J_{HP} unresolved, 2H; Hα) ppm. ^{31}P{^{1}H} NMR (acetone–d$_6$): δ 19.4 (s; PPh$_3$) ppm. MS (MALDI) *m/z* (%) 1867 (40) [M – 3PPh$_3$ – 4CO]$^+$; Anal. Calcd (%) for C$_{118}$H$_{86}$Cl$_2$N$_4$O$_{12}$Os$_2$P$_4$Re$_2$S$_2$·5CH$_2$Cl$_2$ (M$_w$ = 3188.43, M$_w$ = 2763.77 in absence of solvation): C 46.3, H 3.0, N 1.8 %. Found: C 46.5, H 2.9, N 2.2 %.

[(dppf){AuSC$_6$H$_4$CO$_2$Os(CH=CH-bpyReCl(CO)$_3$)(CO)(PPh$_3$)$_2$}$_2$] (15)

Using the same procedure employed to prepare **11**, with [dppf(AuSC$_6$H$_4$CO$_2$H)$_2$] (23 mg, 0.018 mmol), sodium methoxide (2.0 mg, 0.037 mmol) and [Os{CH=CH–bypReCl(CO)$_3$}Cl(CO)(BTD)(PPh$_3$)$_2$] (50 mg, 0.036 mmol) provided an orange solid. Yield: 47 mg (70%). IR (solid state): 2016 (ν_{CO}), 1886 (ν_{CO}), 1586 ($\nu_{C\text{-}O}$), 1534, 1469, 1420, 1355, 1168, 1095, 869, 744, 692 cm^{-1}. ^{1}H NMR (CD$_2$Cl$_2$): δ 4.30, 4.64 (s(br) x 2, 2 x 4H; C$_5$H$_4$), 5.63 (d, J_{HH} = 15.8 Hz, 2H; Hβ), 6.89 (d x 2, J_{HH} = 8.4 Hz, 4H; C_6H_4), 6.96 (dd, J_{HH} = 8.6, 1.9 Hz, 2H; bpy), 7.25 (d x 2, J_{HH} = 8.4 Hz, 4H; C_6H_4), 7.30 – 7.62 (m, 80H + 4H; C_6H_5 + bpy), 7.75 (d, J_{HH} = 8.6 Hz, 2H; bpy), 7.92 (s, 2H; bpy), 8.01 (m, 4H; bpy), 8.95 (d, J_{HH} = 5.5 Hz, 2H; bpy), 9.38 (dt, J_{HH} = 15.8 Hz, J_{HP} = 1.8 Hz, 2H; Hα) ppm. $^{31}P\{^1H\}$ NMR (CD_2Cl_2): δ 19.0 (s; PPh_3), 32.5 (s(br); dppf) ppm. MS (MALDI) *m/z* (%) 3537 (100) [M – Cl – 5CO]$^+$; Anal. Calcd (%) for $C_{152}H_{114}Au_2Cl_2FeN_4O_{12}Os_2P_6Re_2S_2$ (M_w = 3712.08): C 49.2, H 3.1, N 1.5 %. Found: C 49.2, H 3.2, N 1.6 %.

[(Ph$_3$P)Au(SC$_6$H$_4$CO$_2$-4)Ru(CH=CHC$_6$H$_4$Me-4)(CO)(PPh$_3$)$_2$] (16)

Using the same procedure as employed for the preparation of **4**, with [Au($SC_6H_4CO_2H$)(PPh_3)] (15 mg, 0.025 mmol), sodium methoxide (1.4 mg, 0.026 mmol) and [Ru(CH=CHC_6H_4Me–4)Cl(CO)(BTD)(PPh_3)$_2$] (23 mg, 0.025 mmol) provided a light yellow solid. Yield: 22 mg (64%). IR (solid state): 1908 (ν_{CO}), 1586 ($\nu_{C\text{-}O}$), 1481, 1425, 1175, 1095, 863, 742, 692 cm^{-1}. ^1H NMR (CD_2Cl_2): δ 2.23 (s, 3H; CH_3), 5.83 (d, J_{HH} = 15.4, 1H; Hβ), 6.39, 6.83 (d x 2, J_{HH} = 8.0 Hz, 4H; C_6H_4Me), 6.85, 7.20 (d x 2, J_{HH} = 8.3 Hz, 4H; SC_6H_4), 7.32 – 7.40, 7.46 – 7.63 (m x 2, 45H; C_6H_5), 7.85 (dt, J_{HH} = 15.4, J_{HP} = 2.6 Hz, 1H; Hα) ppm. $^{13}C\{^1H\}$ NMR (CD_2Cl_2, 500 MHz): δ 207.1 (t, J_{PC} = 15.3 Hz, CO), 178.2 (s, CO_2), 153.5 (t, J_{PC} = 11.7 Hz, Cα), 147.6 (s, CS), 138.6 (s, $C^{1/4}$-C_6H_4), 134.7 (t^v, J_{PC} = 5.8 Hz, *o/m*-RuPC_6H_5), 134.5 (d, J_{PC} = 13.7 Hz, *o/m*-AuPC_6H_5), 133.8 (t(br), J_{PC} unresolved, Cβ), 133.3 (s, $C^{1/4}$-C_6H_4), 132.2 (s, *p*-AuPC_6H_5), 131.9 (t^v, J_{PC} = 21.4 Hz, *ipso*-RuPC_6H_5), 130.7 (s, *o/m*-C_6H_4), 130.5 (s, $C^{1/4}$-C_6H_4), 130.1 (s, *p*-RuPC_6H_5), 129.7 (d, J_{PC} = 11.2 Hz, *o/m*-AuPC_6H_5), 129.3 (d, J_{PC} = 25.3 Hz, *ipso*-AuPC_6H_5), 128.6 (s, *o/m*-C_6H_4), 128.3 (t^v, J_{PC} = 5.6 Hz, *o/m*-RuPC_6H_5), 127.9, 124.5 (s x 2, *o/m*-C_6H_4), 20.9 (s,CH_3) ppm. $^{31}P\{^1H\}$ NMR (CD_2Cl_2): δ 37.5 (s; RuPPh_3), 38.7 (s; AuPPh_3). MS (ES +ve) *m/z* (%) 1405 (5) [M + Na]$^+$; Anal. Calcd (%) for $C_{71}H_{58}AuO_3P_3RuS$ (M_w = 1382.24): C 61.7, H 4.2%. Found: C 61.7, H 4.1 %.

[(IDip)Au(SC$_6$H$_4$CO$_2$-4)Ru(CH=CHC$_6$H$_4$Me-4)(CO)(PPh$_3$)$_2$] (17)

Employing the same procedure as used for the synthesis of **4**, with [Au($SC_6H_4CO_2H$)(IDip)] (15 mg, 0.020 mmol), sodium methoxide (1.1 mg, 0.020 mmol) and [Ru(CH=CHC_6H_4Me–4)Cl(CO)(BTD)(PPh_3)$_2$] (20 mg, 0.020 mmol) provided a yellow solid. Yield: 21 mg (70%). IR (solid state): 2960, 1923 (ν_{CO}), 1723, 1587 ($\nu_{C\text{-}O}$), 1480, 1417, 1260, 1172, 1093, 801, 746, 691 cm^{-1}. ^1H NMR (CD_2Cl_2): δ 1.28, 1.34 (d x 2, J_{HH} = 6.9 Hz, 2 x 12H; IDip-CH_3), 2.23 (s, 3H; tolyl-CH_3), 2.65 (sep, J_{HH} = 6.9 Hz, 4H; *CH*Me_2), 5.82 (d, J_{HH} = 15.3 Hz, 1H; Hβ), 6.41

(d, J_{HH} = 8.0 Hz, 2H; C_6H_4), 6.43 (d, J_{HH} = 8.3 Hz, 2H; C_6H_4), 6.58 (d, J_{HH} = 8.3 Hz, 2H; C_6H_4), 6.84 (d, J_{HH} = 8.0 Hz, 2H; C_6H_4), 7.29 (s, 2H; NCH), 7.33 – 7.41, 7.48 – 7.52 (m x 2, 30H + 4H; C_6H_5 + *m*-C_6H_3), 7.60 (t, J_{HH} = 7.8 Hz, 2H; *p*-C_6H_3), 7.88 (dt, J_{HH} = 15.3, J_{HP} = 2.7 Hz, 1H; Hα) ppm. $^{31}P\{^1H\}$ NMR (CD_2Cl_2): δ 37.4 (s; PPh_3). MS (ES +ve) *m/z* (%) 1554 (1) $[M + 2Na]^+$, 1269 (50) $[M – PPh_3 + Na]^+$. Anal. Calcd (%) for $C_{80}H_{79}AuN_2O_3P_2RuS$ (M_w = 1508.54): C 63.7, H 5.3, N 1.9 %. Found: C 63.5, H 5.2, N 2.1 %.

[(Ph$_3$P)Au(SC$_6$H$_4$CO$_2$-4)Ru(C(C≡CPh)=CHPh)(CO)(PPh$_3$)$_2$] (18)

Employing the same procedure as used for the synthesis of **4**, with $[Au(SC_6H_4CO_2H)(PPh_3)]$ (35 mg, 0.057 mmol), sodium methoxide (3.1 mg, 0.057 mmol) and $[Ru(C(C{\equiv}CPh){=}CHPh)(CO)(PPh_3)_2]$ (50 mg, 0.057 mmol) provided a yellow solid. Yield: 57 mg (68%). IR (solid state): 2163 ($\nu_{C\equiv C}$), 1919 (ν_{CO}), 1588 ($\nu_{C\text{-}O}$), 1481, 1433, 1419, 1173, 1094, 864, 742, 690 cm^{-1}. ^1H NMR (CD_2Cl_2): δ 6.08 (s(br), 1H; CHPh), 6.86 (d, J_{HH} = 8.1 Hz, 2H; $C_6\mathit{H}_4$Me), 7.00, 7.10, 7.17 – 7.72 (m x 3, 42H; $C_6\mathit{H}_4$Me + CC_6H_5 + PC_6H_5) ppm. $^{13}C\{^1H\}$ NMR (CD_2Cl_2, 500 MHz): δ 207.4 (t, J_{PC} = 15.0 Hz, CO), 178.0 (s, CO_2), 147.6 (s, CS), 140.4 (t(br), J_{PC} unresolved, Cα), 134.9 (t^v, J_{PC} = 5.9 Hz, *o/m*-RuPC_6H_5), 134.5 (d, J_{PC} = 13.6 Hz, *o/m*-AuPC_6H_5), 132.2 (s, *p*-AuPC_6H_5), 131.7 (s, *o/m*-C_6H_4), 131.2 (t^v, J_{PC} = 21.6 Hz, *ipso*-RuPC_6H_5), 130.6 (s, *o/m*-C_6H_4), 130.1 (s, *p*-RuPC_6H_5), 129.7 (d, J_{PC} = 25.7 Hz, *ipso*-AuPC_6H_5), 129.6 (d, J_{PC} = 11.2 Hz, *o/m*-AuPC_6H_5), 128.9 (s, quaternary-C), 128.5 (s, $C\mathit{C}_6H_5$), 128.1 (t^v, J_{PC} = 5.0 Hz, *o/m*-RuPC_6H_5), 127.8, 127.4 (s x 2, $C\mathit{C}_6H_5$), 127.3 (s, quaternary-C), 126.6 (t(br), J_{PC} unresolved, Cβ), 124.9 (s, $C\mathit{C}_6H_5$) ppm. $^{31}P\{^1H\}$ NMR (CD_2Cl_2): δ 37.5 (s; RuPPh_3), 37.1 (s; AuPPh_3). MS (ES +ve) *m/z* (%) 1469 (6) $[M]^+$; Anal. Calcd (%) for $C_{78}H_{60}AuO_3P_3RuS$ (M_w = 1468.33): C 63.8, H 4.1%. Found: C 63.7, H 4.0 %.

[(Ph$_3$P)Au(SC$_6$H$_4$CO$_2$-4)Os(CH=CHC$_6$H$_4$Me-4)(CO)(PPh$_3$)$_2$] (19)

Using the same procedure as employed to prepare **4**, with $[Au(SC_6H_4CO_2H)(PPh_3)]$ (15 mg, 0.025 mmol), sodium methoxide (1.4 mg, 0.026 mmol) and $[Os(CH{=}CHC_6H_4Me–4)Cl(CO)(BTD)(PPh_3)_2]$ (25 mg, 0.024 mmol) provided a yellow solid. Yield: 27 mg (77%). IR (solid state): 1893 (ν_{CO}), 1586 ($\nu_{C\text{-}O}$), 1480, 1430, 1176, 1096, 868, 742, 692 cm^{-1}. ^1H NMR (CD_2Cl_2): δ 2.22 (s, 3H; CH_3), 5.69 (d, J_{HH} = 15.9 Hz, 1H; Hβ), 6.38 (d, J_{HH} = 8.0 Hz, 2H; $C_6\mathit{H}_4$Me), 6.81 (d, J_{HH} = 8.3 Hz, 2H; SC_6H_4), 6.82 (d, J_{HH} = 8.0 Hz, 2H; $C_6\mathit{H}_4$Me), 7.22 (d, J_{HH} = 8.3 Hz, 2H; SC_6H_4), 7.33 – 7.63 (m, 45H; C_6H_5), 8.21 (dt, J_{HH} = 15.9 Hz, J_{HH} = 1.9 Hz, 1H; Hα) ppm. $^{31}P\{^1H\}$ NMR (CD_2Cl_2): δ 18.3 (s; OsPPh_3), 38.8 (s; AuPPh_3). MS (ES

+ve) *m/z* (%) 1471 (2) $[M]^+$; Anal. Calcd (%) for $C_{71}H_{58}AuO_3OsP_3S$ (M_w = 1471.40): C 58.0, H 4.0 %. Found: C 57.9, H 3.9 %.

[(IDip)Au(SC$_6$H$_4$CO$_2$-4)Os(CH=CHC$_6$H$_4$Me-4)(CO)(PPh$_3$)$_2$] (20)

Employing the same procedure used to synthesize **4**, with [Au(SC$_6$H$_4$CO$_2$H)(IDip)] (15 mg, 0.020 mmol), sodium methoxide (1.1 mg, 0.020 mmol) and [Os(CH=CHC$_6$H$_4$Me–4)Cl(CO)(BTD)(PPh$_3$)$_2$] (21 mg, 0.020 mmol) provided a pale yellow solid. Yield: 17 mg (53%). IR (solid state): 2959, 1891 (ν_{CO}), 1587 ($\nu_{C\text{-}O}$), 1479, 1419, 1174, 1095, 868, 803, 745, 693 cm^{-1}. ^{1}H NMR (CD$_2$Cl$_2$): δ 1.28, 1.34 (d x 2, J_{HH} = 6.8 Hz, 2 x 12H; IDip-CH$_3$), 2.22 (s, 3H; tolyl-CH$_3$), 2.64 (sep, J_{HH} = 6.9 Hz, 4H; *CH*Me$_2$), 5.68 (d, J_{HH} = 15.9 Hz, 1H; Hβ), 6.40 (d, J_{HH} = 7.8 Hz, 2H; C$_6$*H*$_4$Me), 6.45, 6.53 (d x 2, J_{HH} = 8.3 Hz, 2 x 2H; SC$_6$H$_4$), 6.82 (d, J_{HH} = 7.8 Hz, 2H; C$_6$*H*$_4$Me), 7.29 (s, 2H; NCH), 7.33 – 7.51 (m, 30H + 4H; C$_6$H$_5$ + *m*-C$_6$H$_3$), 7.60 (t, J_{HH} = 7.8 Hz, 2H; *p*-C$_6$H$_3$), 8.23 (dt, J_{HH} = 15.9 Hz, J_{HP} = 2.0 Hz, 1H; Hα) ppm. ^{31}P{^{1}H} NMR (CD$_2$Cl$_2$): δ 18.0 (s; PPh$_3$) ppm. MS (ES +ve) *m/z* (%) 1599 (27) $[M + H]^+$; Anal. Calcd (%) for $C_{80}H_{79}AuN_2O_3OsP_2S$ (M_w = 1597.71): C 60.1, H 5.0, N 1.8 %. Found: C 59.9, H 4.9, N 1.8 %.

[(Ph$_3$P)Au(SC$_6$H$_4$CO$_2$-4)Ru{CH=CH-bpyReCl(CO)$_3$}(CO)(PPh$_3$)$_2$] (21)

Employing the same procedure used to synthesize **4**, with [Au(SC$_6$H$_4$CO$_2$H)(PPh$_3$)] (23 mg, 0.038 mmol), sodium methoxide (2.1 mg, 0.039 mmol) and [Ru{CH=CH-bpyReCl(CO)$_3$}Cl(CO)(BTD)(PPh$_3$)$_2$] (50 mg, 0.038 mmol) provided an orange solid. Yield: 61 mg (92%). IR (solid state): 2016 (ν_{CO}), 1909 (ν_{CO}), 1885 (ν_{CO}), 1587 ($\nu_{C\text{-}O}$), 1535, 1481, 1434, 1419, 1176, 1095, 862, 744, 692 cm^{-1}. ^{1}H NMR (CD$_2$Cl$_2$): δ 5.78 (d, J_{HH} = 15.6 Hz, 1H; Hβ), 6.92 (d, J_{HH} = 8.5 Hz, 2H; SC$_6$H$_4$), 6.98 (dd, J_{HH} = 8.6, 2.0 Hz, 1H; bpy), 7.21 (d, J_{HH} = 8.5 Hz, 2H; SC$_6$H$_4$), 7.36 – 7.61 (m, 45H; C$_6$H$_5$), 7.78 (d, J_{HH} = 8.5 Hz, 2H; bpy), 7.92 (s(br), 1H; bpy), 8.02 (m, 2H; bpy), 8.92 (dt, J_{HH} = 15.6 Hz, J_{HH} = 2.5 Hz, 1H; Hα), 8.97 (d, J_{HH} = 5.4 Hz, 1H; bpy) ppm. ^{31}P{^{1}H} NMR (CD$_2$Cl$_2$): δ 37.9 (s; RuPPh$_3$), 38.0 (s; AuPPh$_3$). MS (ES +ve) *m/z* (%) 1753 (22) $[M]^+$, 1793 (62) $[M + K]^+$; Anal. Calcd (%) for $C_{77}H_{58}AuClN_2O_6P_3ReRuS$ (M_w = 1751.98): C 52.8, H 3.3, N 1.6 %. Found: C 52.6, H 3.4, N 1.7 %.

[(IDip)Au($SC_6H_4CO_2$-4)Os{CH=CH-bpyReCl$(CO)_3$}(CO)$(PPh_3)_2$] (22)

Using the same procedure employed for the preparation of **4**, with [Au($SC_6H_4CO_2H$)(IDip)] (13 mg, 0.018 mmol), sodium methoxide (1.0 mg, 0.019 mmol) and [Os{CH=CH–bpyReCl$(CO)_3$}Cl(CO)(BTD)$(PPh_3)_2$] (24 mg, 0.017 mmol) provided an orange solid. Yield: 23 mg (69%). IR: 2964, 2014 (ν_{CO}), 1882 (ν_{CO}), 1586 ($\nu_{C\text{-}O}$), 1532, 1469, 1434, 1418, 1239, 1168, 1094, 802, 744, 692 cm^{-1}. ^1H NMR (CD_2Cl_2): δ 1.30, 1.35 (d x 2, J_{HH} = 6.8 Hz, 2 x 12H; IDip-CH_3), 2.66 (sep, J_{HH} = 6.9 Hz, 4H; *CH*Me_2), 5.64 (d, J_{HH} = 15.7 Hz, 1H; Hβ), 6.47, 6.59 (d x 2, J_{HH} = 8.4 Hz, 2 x 2H; SC_6H_4), 6.98 (dd, J_{HH} = 8.6, 1.8 Hz, 1H; bpy), 7.31 (s, 2H; NCH), 7.27 – 7.50 (m, 30H + 4H + 1H; C_6H_5 + *m*-C_6H_3 + bpy), 7.64 (t, J_{HH} = 8.6 Hz, 2H; *p*-C_6H_3), 7.77 (d, J_{HH} = 8.6 Hz, 1H; bpy), 7.95 (s, 1H; bpy), 8.02 (m, 2H; bpy), 8.96 (d, J_{HH} = 5.6 Hz, 1H; bpy), 9.43 (dt, J_{HH} = 15.7 Hz, J_{HP} = 1.8 Hz, 1H; Hα) ppm. $^{31}P\{^1H\}$ NMR (CD_2Cl_2): δ 18.9 (s, PPh_3) ppm. MS (ES +ve) *m/z* (%) 1967 (2) $[M]^+$; Anal. Calcd (%) for $C_{86}H_{79}AuClN_4O_6OsP_2ReS.CH_2Cl_2$ (M_w = 2052.37, M_w = 1967.44 in absence of solvation): C 50.9, H 4.0, N 2.7. Found: C 50.6, H 3.8, N 2.8 %.

$Au^{2.9}$@[$SC_6H_4CO_2Ru(dppm)_2$]PF_6 (NP1)

A solution of tetracholoroauric acid trihydrate (50.0 mg, 0.127 mmol) in methanol (10 mL) was added to a solution of **2** (149 mg, 0.064 mmol) in methanol (5 mL). The mixture was stirred for 30 minutes at room temperature and then cooled to 4 °C. A fresh solution of sodium borohydride (40.4 mg, 1.063 mmol) in water (3 mL) was then added dropwise. The color of the solution changed from yellow to dark brown indicating the formation of nanoparticles. The mixture was stirred for a further 3 hours at 10 °C. The supernatant was removed by centrifugation and the brown solid was washed with water (3 x 10 mL) and dichloromethane (10 mL) to remove unattached surface units. The black nanoparticles (40 mg) were dried under vacuum and stored under nitrogen. IR (solid state): 1575 ($\nu_{C=O}$), 1483, 1435, 1096, 999, 817 (ν_{PF}), 724, 685 cm^{-1}; ^1H NMR (dmso-d_6, 500 MHz): δ 4.44, 5.76 (m x 2, 2 x 2H; PCH_2P), 6.59 (m, 4H; C_6H_5), 7.08, 7.24, 7.37, 7.53, 7.70, 7.93 (m x 6, 36 H + 4 H; C_6H_5 + C_6H_4) ppm; $^{31}P\{^1H\}$ NMR (dmso-d_6, 500 MHz): δ −18.6, −3.2 (pseudoquartet x 2, J_{PP} = 35.7 Hz; dppm) ppm. TEM: Analysis of over 200 nanoparticles gave a size of 2.9 ± 0.2 nm. EDS: Confirmed the presence of gold and ruthenium and indicated presence of sulfur, phosphorus, oxygen and fluorine. TGA: 37.8% surface units, 62.2% gold and ruthenium ($Au_{8.4}(SC_6H_4CO_2Ru(dppm)_2)PF_6$).

$Au^{11.9}@[SC_6H_4CO_2Ru(dppm)_2]PF_6$ (NP2)

Tetrachloroauric acid trihydrate (20 mg, 0.051 mmol) was dissolved in ultrapure water (60 mL). The solution was heated to reflux for 20 minutes. A pre-heated aqueous solution (4 mL) of trisodium citrate (52.7 mg, 0.204 mmol) was added. The heating source was quickly removed and the stirred solution was left to cool to room temperature. A mixture of methanol and acetonitrile solution (3 mL) of **2** (179 mg, 0.077 mmol) was added and the mixture stirred for 3 hours at room temperature after which it was stored at 4ºC overnight in order to allow the nanoparticles formed to settle. The supernatant was removed and the nanoparticles were washed with water (3 x 10 mL) and centrifuged. Methanol (3 x 10 mL) and dichloromethane (10 mL) washes were employed to remove unattached surface units. The resulting dark blue solid (112 mg) isolated was dried under vacuum and stored under nitrogen. IR (solid state): 1586 ($\nu_{C\text{-}O}$), 1485, 1436, 1098, 1000, 834 (ν_{PF}), 735, 698 cm^{-1}; ^1H NMR (dmso-d_6, 500 MHz): δ 4.43, 5.74 (m x 2, 2 x 2H; PCH_2P), 6.61 (m, 4H; C_6H_5), 7.10, 7.26, 7.38, 7.54, 7.72, 7.94 (m x 6, 36H + 4H; C_6H_5 + C_6H_4) ppm; $^{31}P\{^1H\}$ NMR (dmso-d_6, 500 MHz): δ −18.6, −3.2 (pseudotriplet x 2, J_{PP} = 35.6 Hz; dppm) ppm. TEM: Analysis of over 200 nanoparticles gave a size of 11.9 ± 0.9 nm. EDS: Confirmed the presence of gold and ruthenium and indicated presence of sulfur, phosphorus, oxygen and fluorine. TGA: 42.5% surface units, 57.5% gold and ruthenium ($Au_{6.8}(SC_6H_4CO_2Ru(dppm)_2)PF_6$).

$Au@[SC_6H_4CO_2H]$ (NP3)

Heating PPN[$Au(SC_6H_4CO_2H\text{-}4)_2$] (PPN = bis(triphenylphosphine)iminium) (25 mg, 0.024 mmol) in acetone (5 mL) with excess sodium borohydride (18 mg, 0.476 mmol) results in the darkening of the solution and the formation of a fine black solid, which were washed with water (3 x 10 mL) and Methanol (2 x 10 mL) and centrifuged. The resulting black solid (11 mg) was dried under vacuum. IR (solid state): 1587 ($\nu_{C\text{-}O}$), 1482, 1436, 1096 cm^{-1}; ^1H NMR (dmso-d_6): δ 7.45, 7.56 (m(br) x 2, 4H; C_6H_4) ppm; TEM: Analysis of over 100 nanoparticles gave a size of 4.1 ± 0.7 nm. EDS: Confirmed the presence of gold and sulfur.

$Pd@[SC_6H_4CO_2Ru(dppm)_2]PF_6$ (NP4)

[$PdCl_2(NCMe)_2$] (13 mg, 0.050 mmol) and tetraoctylammonium bromide (109 mg, 0.200 mmol) were dissolved in dry tetrahydrofuran (10 mL) under an inert atmosphere. After 10 minutes stirring, lithium triethylborohydride (1 M tetrahydrofuran solution, 0.15 mL, 3 eq.) was added with vigorous stirring. The solution faded from red to black indicating the formation of nanoparticles. After 30 minutes, a solution of **2** (117 mg, 0.050 mmol) in a 2:1 mixture of dry tetrahydrofuran and dry acetonitrile was added (3 mL). The mixture was stirred overnight at room temperature. The mixture was then centrifuged and the supernatant removed. The remaining solid was washed with methanol (2 x 10 mL) and acetone (2 x 10 mL). The resultant black solid (16.5 mg) was dried under vacuum and stored under nitrogen. It was found to be insoluble in all available deuterated solvents so no NMR data could be recorded. IR (solid state): 1585 ($\nu_{C\text{-}O}$), 1485, 1435, 1098, 828 (ν_{PF}) cm^{-1}. TEM: Analysis of over 200 nanoparticles gave a size of 2.2 ± 0.2 nm. EDS: Confirmed the presence of palladium and ruthenium and indicated presence of sulfur, phosphorus, oxygen and fluorine. TGA: 38.4% surface units, 61.6% palladium and ruthenium ($Pd_{15.1}(SC_6H_4CO_2Ru(dppm)_2)PF_6$).

Acknowledgements

We are grateful to the Wellcome Trust for the award of a Networks of Excellence award (M.N.W). F.G.R. would like to thank the Ministerio de Ciencia e Innovación, Spain, for provision of funding (grants CTQ2009-12520 and CTQ2010-15292). K.A.J. is grateful to the Ministry of Higher Education, Malaysia for a scholarship on the IPTA Academic Training Scheme and for an Academic Staff Scholarship from the Universiti Teknologi MARA, Malaysia.

References

(1) a) He, X.; Herranz, F.; Cheng, E. C.-C.; Vilar, R.; Yam, V. W.-W. Design, synthesis, photophysics, and anion-binding studies of bis(dicyclohexylphosphino)methane-containing dinuclear gold(I) thiolate complexes with urea receptors. *Chem. Eur. J.* **2010**, *16*, 9123–9131; b) Mendy, J. S.; Saeed, M. A.; Fronczek, F. R.; Powell, D. R.; Hossain, Md. A. Anion recognition and sensing by a new macrocyclic dinuclear copper(II) complex: A selective receptor for iodide. *Inorg. Chem.* **2010**, *49*, 7223–7225; c) Saeed, M. A.; Powell, D. R.; Hossain, M. A. Fluorescent detection of phosphate anion by a highly selective chemosensor in water. *Tet. Lett.* **2010**, *51*, 4904–4907.

(2) a) Livramento, J. B.; Tóth, E.; Sour, A.; Borel, A.; Merbach, A. E.; Ruloff, R. High relaxivity confined to a small molecular space: A metallostar-based, potential MRI

contrast agent. *Angew. Chem. Int. Ed.* **2005**, *44*, 1480-1484; b) Livramento, J. B.; Sour, A.; Borel, A.; Merbach, A. E.; Tóth, E. A starburst-shaped heterometallic compound incorporating six densely packed Gd^{3+} ions. *Chem. Eur. J.* **2006**, *12*, 989-1003; c) Moriggi, L.; Aebischer, A.; Cannizzo, C.; Sour, A.; Borel, A.; Bunzli, J.-C. G.; Helm, L. A ruthenium-based metallostar: synthesis, sensitized luminescence and ^{1}H relaxivity. *Dalton Trans*. **2009**, 2088-2095; d) Kasala, D.; Lin, T.-S.; Chen, C.-Y.; Liu, G.-C.; Kao, C.-L.; Cheng, T.-L.; Wang, Y.-M. $[Gd(Try\text{-}TTDA)(H_2O)]^{2-}$***:*** A new MRI contrast agent for copper ion sensing. *Dalton Trans*. **2011**, *40*, 5018-5025; e) Mieville, P.; Jaccard, H.; Reviriego, F.; Tripier, R.; Helm, L. Synthesis, complexation and NMR relaxation properties of Gd^{3+} complexes of $Mes(DO3A)_3$. *Dalton Trans.* **2011**, *40*, 4260-4267; f) Dehaen, G.; Verwilst, P.; Eliseeva, S. V.; Laurent, S.; Vander Elst, L.; Muller, R. N.; De Borggraeve, W. M.; Binnemans, K.; Parac-Vogt, T. N. A heterobimetallic ruthenium–gadolinium complex as a potential agent for bimodal imaging. *Inorg. Chem.* **2011**, *50*, 10005–10014; g) Dehaen, G.; Eliseeva, S. V.; Kimpe, K.; Laurent, S.; Vander Elst, L.; Muller, R. N.; Dehaen, W.; Binnemans, K.; Parac-Vogt, T. N. A self-assembled complex with a titanium(IV) catecholate core as a potential bimodal contrast agent. *Chem. Eur. J.* **2012**, *18*, 293–302; h) Verwilst, P.; Eliseeva, S. V.; Vander Elst, L. Burtea, C.; Laurent, S.; Petoud, S.; Muller, R. N.; Parac-Vogt, T. N.; De Borggraeve, W. M. A tripodal ruthenium–gadolinium metallostar as a potential $\alpha_v\beta_3$ integrin specific bimodal imaging contrast agent. *Inorg. Chem.* **2012**, *51*, 6405−6411; i) Dehaen, G.; Eliseeva, S. V.; Verwilst, P.; Laurent, S.; Vander Elst, L.; Muller, R. N.; De Borggraeve, W.; Binnemans, K.; Parac-Vogt, T. N. Tetranuclear d-f metallostars: Synthesis, relaxometric, and luminescent properties. *Inorg. Chem.* **2012**, *51*, 8775−8783; j) Sung, S.; Holmes, H.; Wainwright, L.; Toscani, A.; Stasiuk, G. J.; White, A. J. P.; Bell, J. D.; Wilton-Ely, J. D. E. T. Multimetallic complexes and functionalized gold nanoparticles based on a combination of d- and f-elements. *Inorg. Chem.* **2014**, *53*, 1989-2005.

(3) a) Shibasaki, M.; Kanai, M.; Matsunaga, S.; Kumagai, N. Recent progress in asymmetric bifunctional catalysis using multimetallic systems. *Acc. Chem. Res.* **2009**, *42*, 1117-1127; b) Weber, M.; Klein, J. E. M. N.; Miehlich, B.; Frey, W.; Peters, R. Monomeric ferrocene bis-imidazoline bis-palladacycles: Variation of Pd–Pd distances by an interplay of metallophilic, dispersive, and coulombic interactions. *Organometallics* **2013**, *32*, 5810-5817; c) Sasai, H.; Suzuki, T.; Arai, S.; Arai, T.; Shibasaki, M. Basic character of rare earth metal alkoxides. Utilization in catalytic

carbon-carbon bond-forming reactions and catalytic asymmetric nitroaldol reactions. *J. Am. Chem. Soc.* **1992**, *114*, 4418-4420; d) Ho, J. H. H.; Wagler, J.; Willis, A. C.; Messerle, B. A. Synthesis and structures of homo- and heterobimetallic rhodium(I) and/or iridium(I) complexes of binucleating bis(1-pyrazolyl)methane ligands. *Dalton Trans*. **2011**, *40*, 11031-11042; e) Lee, W.-Z.; Wang, T.-L.; Chang, H.-C.; Chen, Y.-T.; Kuo, T.-S. A bioinspired Zn^{II}/Fe^{III} heterobimetallic catalyst for thia-michael addition. *Organometallics* **2012**, *31*, 4106-4109; f) Yamaguchi, Y.; Yamanishi, K.; Kondo, M.; Tsukada, N. Synthesis of dinuclear (μ-η^3-allyl)palladium(I) and -platinum(I) complexes supported by chelate-bridging ligands. *Organometallics* **2013**, *32*, 4837-4842; g) Wu, B.; Gallucci, J. C.; Parquette, J. R.; RajanBabu, T. V. Bimetallic catalysis in the highly enantioselective ring–opening reactions of aziridines. *Chem. Sci.* **2014**, *5*, 1102-1117.

(4) Jabri, E.; Carr, M. B.; Hausinger, R. P.; Karplus, P. A. The crystal structure of urease from Klebsiella aerogenes. *Science* **1995**, *268*, 998-1004.

(5) Low, P. J. Twists and turns: Studies of the complexes and properties of bimetallic complexes featuring phenylene ethynylene and related bridging ligands. Low, P. J. *Coord. Chem. Rev.* **2013**, *257*, 1507–1532.

(6) a) Eddaoudi, H. Li, M.; O'Keeffe, M.; Yaghi, O. Design and synthesis of an exceptionally stable and highly porous metal-organic framework. *Nature* **1999**, *402*, 276–279. b) Long, J. R.; Yaghi, O. M. The pervasive chemistry of metal–organic frameworks. *Chem. Soc. Rev.* **2009**, *38*, 1213–1214 and subsequent reviews in the same issue; c) Janiak, C.; Vieth, J. K. MOFs, MILs and more: concepts, properties and applications for porous coordination networks (PCNs). *New J. Chem.* **2010**, *34*, 2366–2388; d) Janiak, C. Engineering coordination polymers towards applications. *Dalton Trans.* **2003**, 2781–2804; e) Arora, H.; Mukherjee, R. Coordination polymers using (2-pyridyl)alkylamine-appended carboxylates: magnetic properties. *New J. Chem.* **2010**, *34*, 2357–2365.

(7) a) Toscani, A.; Heliövaara, E. K.; Hena, J. B.; White, A. J. P.; Wilton-Ely, J. D. E. T. Multimetallic alkenyl complexes bearing macrocyclic dithiocarbamate ligands. *Organometallics* **2015**, *34*, 494−505; b) Lin, Y. H.; Duclaux, L.; Gonzàlez de Rivera, F.; Thompson, A. L.; Wilton-Ely, J. D. E. T. The pentynoate ligand as a building block for multimetallic systems. *Eur. J. Inorg. Chem.* **2014**, 2065-2072; c) Hurtubise, V. L.; McArdle, J. M.; Naeem, S.; Toscani, A.; White, A. J. P.; Long, N. J.; Wilton-Ely, J. D. E. T. Multimetallic complexes and functionalized nanoparticles based on

unsymmetrical dithiocarbamate ligands with allyl and propargyl functionality. *Inorg. Chem.* **2014**, *53*, 11740−11748; d) Naeem, S.; Ribes, A.; White, A. J. P.; Haque, M. N.; Holt, K. B.; Wilton-Ely, J. D. E. T. Multimetallic complexes and functionalized nanoparticles based on oxygen-and nitrogen-donor combinations. *Inorg. Chem.* **2013**, *52*, 4700-4713; e) Lin, Y. H.; Leung, N. H.; Holt, K. B.; Thompson, A. L.; Wilton-Ely, J. D. E. T. Bimetallic complexes based on carboxylate and xanthate ligands: Synthesis and electrochemical investigations. *Dalton Trans.* **2009**, 7891-7901; f) Sherwood, R.; Gonzàlez de Rivera, F.; Wan, J. H.; Zhang, Q.; White, A. J. P.; Rossell, O.; Hogarth, G.; Wilton-Ely, J. D. E. T. Multimetallic complexes based on a diphosphine-dithiocarbamate “Janus” ligand. *Inorg. Chem.* **2015**, *54*, 4222−4230.

(8) a) Packheiser, R.; Ecorchard, P.; Rüffer, T.; Walfort, B.; Lang, H. Mixed heterotri- to heteropentametallic transition-metal complexes: Synthesis, characterization and electrochemical behavior. *Eur. J. Inorg. Chem.* **2008**, 4152–4165; b) Packheiser, R.; Jakob, A.; Ecorchard, P.; Walfort, B.; Lang, H. Diphenylphosphinoferrocene gold(I) acetylides: Synthesis of heterotri-and heterotetrametallic transition metal complexes. *Organometallics* **2008**, *27*, 1214–1226; c) Packheiser, R.; Ecorchard, P.; Rüffer, T.; Lang, H. Mixed-transition-metal acetylides: Synthesis and characterization of complexes with up to six different transition metals connected by carbon-rich bridging units. *Chem. Eur. J.* **2008**, *14*, 4948–4960; d) Packheiser, R.; Ecorchard, P.; Walfort, B.; Lang, H. Heterotrimetallic and heterotetrametallic transition metal complexes. *J. Organomet. Chem.* **2008**, *693*, 933–946; e) Packheiser, R.; Ecorchard, P.; Rüffer, T.; Lohan, M.; Bräuer, B.; Justaud, F.; Lapinte, C.; Lang, H. Heterotrimetallic M−M′−M″ transition metal complexes based on 1,3,5-triethynylbenzene: Synthesis, solid state structure, and electrochemical and UV−Vis characterization. EPR analysis of the in situ generated associated radical cations. *Organometallics* **2008**, *27*, 3444–3457; f) Packheiser, R.; Ecorchard, P.; Rüffer, T.; Lang, H. Heteromultimetallic transition metal complexes based on unsymmetrical platinum (II) bis-acetylides. *Organometallics* **2008**, *27*, 3534–3546; g) Lang, H.; Zoufalá, P.; Klaib, S.; del Villar, A.; Rheinwald, G. Synthesis of di-, tri- and tetranuclear platinum(II) and copper(I) acetylide complexes. *J. Organomet. Chem.* **2007**, *692*, 4168–4176; h) Packheiser, R.; Lang, H. The first heterohexametallic transition-metal complex. *Eur. J. Inorg. Chem.* **2007**, 3786–3788; i) Packheiser, R.; Walfort, B.; Lang, H. Heterobi-and heterotrimetallic transition metal complexes with carbon-rich bridging units. *Organometallics* **2006**, *25*, 4579–4587; j) Maurer, J.;

Sarkar, B.; Kaim, W.; Winter, R. F.; Záliš, S. Towards new organometallic wires: Tetraruthenium complexes bridged by phenylenevinylene and vinylpyridine ligands. *Chem. Eur. J.* **2007**, *13*, 10257-10272.

(9) a) Wilton-Ely, J. D. E. T.; Solanki, D.; Hogarth, G. Multifunctional dithiocarbamates as ligands towards the rational synthesis of polymetallic arrays: An example based on a piperizine-derived dithiocarbamate. *Eur. J. Inorg. Chem.* **2005**, 4027-4030; b) Knight, E. R.; Solanki, D.; Hogarth, G.; Holt, K. B.; Thompson, A. L.; Wilton-Ely, J. D. E. T. Multimetallic assemblies using piperazine-based dithiocarbamate building blocks. *Inorg. Chem.* **2008**, *47*, 9642-9653; c) Macgregor, M. J.; Hogarth, G.; Thompson, A. L.; Wilton-Ely, J. D. E. T. Multimetallic arrays: Symmetrical and unsymmetrical bi-, tri-, and tetrametallic organometallic complexes of ruthenium(II) and osmium(II). *Organometallics* **2009**, *28*, 197-208; d) Knight, E. R.; Cowley, A. R.; Hogarth, G.; Wilton-Ely, J. D. E. T. Bifunctional dithiocarbamates: a bridge between coordination chemistry and nanoscale materials. *Dalton Trans.* **2009**, 607-609; e) Knight, E. R.; Leung, N. H.; Lin, Y. H.; Cowley, A. R.; Watkin, D. J.; Thompson, A. L.; Hogarth, G.; Wilton-Ely, J. D. E. T. Multimetallic arrays: Symmetrical bi-, tri- and tetrametallic complexes based on the group 10 metals and the functionalisation of gold nanoparticles with nickel-phosphine surface units. *Dalton Trans.* **2009**, 3688-3697; f) Knight, E. R.; Leung, N. H.; Thompson, A. L.; Hogarth, G.; Wilton-Ely, J. D. E. T. Multimetallic arrays: Bi-, tri-, tetra-, and hexametallic complexes based on gold(I) and gold(III) and the surface functionalization of gold nanoparticles with transition metals. *Inorg. Chem.* **2009**, *48*, 3866-3874; g) Oliver, K.; White, A. J. P.; Hogarth, G.; Wilton-Ely, J. D. E. T. Multimetallic complexes of group 10 and 11 metals based on polydentate dithiocarbamate ligands. *Dalton Trans.* **2011**, *40*, 5852-5864; h) Hogarth, G.; Rainford-Brent, E.-J. C.-R. C. R.; Kabir, S. E.; Richards, I.; Wilton-Ely, J. D. E. T.; Zhang, Q. Functionalised dithiocarbamate complexes: Synthesis and molecular structures of 2-diethylaminoethyl and 3-dimethylaminopropyl dithiocarbamate complexes $[M\{S_2CN(CH_2CH_2NEt_2)_2\}_n]$ and $[M\{S_2CN(CH_2CH_2CH_2NMe_2)_2\}_n]$ (n = 2, M = Ni, Cu, Zn, Pd;n = 3, M = Co). *Inorg. Chim. Acta* **2009**, *362*, 2020–2026; i) Naeem, S.; Ogilvie, E.; White, A. J. P.; Hogarth, G.; Wilton-Ely, J. D. E. T. The functionalisation of ruthenium(II) and osmium(II) alkenyl complexes with amine- and alkoxy-terminated dithiocarbamates. *Dalton Trans.* **2010**, *39*, 4080-4089; j) Bedford, R. B.; Hill, A. F.; Jones, C.; White, A. J. P.;

Williams, D. J.; Wilton-Ely, J. D. E. T. Co-ordinative activation of phosphaalkynes: methyl neopentylidene phosphorane complexes of ruthenium(II); crystal structure of [Ru(MeP=CHBu^t)Cl(I)(CO)(PPh$_3$)$_2$]. *J. Chem. Soc., Dalton Trans.* **1997**, 139-140.

(10) a) Guerrini, L.; Pazos, E.; Penas, C.; Vázquez, M. E.; Mascareñas, J. L.; Alvarez-Puebla, R. A. Highly sensitive SERS quantification of the oncogenic protein c-Jun in cellular extracts. *J. Am. Chem. Soc.* **2013**, *135*, 10314−10317; b) Rowland, C. E.; Belai, N.; Knope, K. E.; Cahill, C. L. Hydrothermal synthesis of disulfide-containing uranyl compounds: in situ ligand synthesis versus direct assembly. *Cryst. Growth Des.* **2010**, *10*, 1390–1398.

(11) a) Signer, R. Über eine Abänderung der Molekulargewichtbestimmungsmethode nach Barger. 34. Mitteilung über hochpolymere Verbindungen. *Annalen* **1930**, *478*, 246; b) Clark, E. P. Signer method for determining molecular weights. *Ind. Eng. Chem., Anal. Ed.* **1941**, *13*, 820; c) Patel, P.; Naeem, S.; White, A. J. P.; Wilton-Ely, J. D. E. T. Synthesis and reactivity of dialkyldithiophosphate complexes of ruthenium(II). *RSC Adv.* **2012**, *2*, 999–1008.

(12) a) Wilton-Ely, J. D. E. T.; Schier, A.; Mitzel, N. W.; Schmidbaur, H. Structural diversity in gold(I) complexes of 4-sulfanylbenzoic acid. *J. Chem. Soc., Dalton Trans*. **2001**, 1058–1062; b) Wilton-Ely, J. D. E. T.; Ehlich, H.; Schier, A.; Schmidbaur, H. The effect of hard and soft donors on structural motifs in (isocyanide)gold(I) complexes. *Helv. Chim. Acta* **2001**, *84*, 3216–3232.

(13) For an overview of alkenyl chemistry of ruthenium(II), see: a) Whittlesey, M. K. in *Comprehensive Organometallic Chemistry III*; Crabtree, R. H.; Mingos, D. M. P.; Bruce, M. I.; Eds.; Elsevier: Oxford, U.K., 2006; Vol. 6; b) Hill, A. F. in *Comprehensive Organometallic Chemistry II*; Abel, E. W.; Stone, F. G. A.; Wilkinson, G.; Eds.; Pergamon Press: Oxford, U.K., 1995; Vol. 7.

(14) Prepared using 2,1,3-benzothiadiazole (BTD) in place of 2,1,3-benzoselenadiazole (BSD) following the procedure reported by Harris, M. C. J.; Hill, A. F. Reactions of ruthenium complex [RuClH(CO)(BSD)(PPh$_3$)$_2$](BSD = benzo-2,1,3-selenadiazole) with alkynes. *Organometallics* **1991**, *10*, 3903-3906.

(15) Hill, A. F.; Wilton-Ely, J. D. E. T. Alkenyl and alkynyl complexes of osmium(II) derived from [OsH(Cl)(CO)(BTD)(PPh$_3$)$_2$] (BTD = 2,1,3-benzothiadiazole). *J. Chem. Soc., Dalton Trans.* **1998**, 3501-3510.

(16) a) Santos, A.; López, J.; Montoya, J.; Noheda, P.; Romero, A.; Echavarren, A. M. Synthesis of new ruthenium (II) carbonyl hydrido, alkenyl, and alkynyl complexes

with chelating diphosphines. *Organometallics* **1994**, *13*, 3605-3615; b) Maurer, J.; Winter, R. F.; Sarkar, B.; Fiedler, J.; Záliš, S. Bridge dominated oxidation of a diruthenium 1, 3-divinylphenylene complex. *Chem. Commun.* **2004**, 1900-1901; c) Maurer, J.; Linseis, M.; Sarkar, B.; Schwederski, B.; Niemeyer, M.; Kaim, W.; Záliš, S.; Anson, C.; Zabel, M.; Winter. R. F. Ruthenium complexes with vinyl, styryl, and vinylpyrenyl ligands: A case of non-innocence in organometallic chemistry. *J. Am. Chem. Soc.* **2008**, *130*, 259-268; d) Scheerer, S.; Rotthowe, N.; Abdel-Rahman, O. S.; He, X.; Rigaut, S.; Kvapilova, H.; Zalis S.; Winter, R. F. Vinyl ruthenium-modified biphenyl and 2, 2′-bipyridines. *Inorg. Chem.* **2015**, *54*, 3387-3402.

(17) a) Moragues, M. E.; Toscani, A.; Sancenón, F.; Martínez-Mañez, R.; White, A. J. P.; Wilton-Ely, J. D. E. T. A chromo-fluorogenic synthetic “canary” for CO detection based on a pyrenylvinyl ruthenium(II) complex. *J. Am. Chem. Soc.* **2014**, *136*, 11930−11933; b) Toscani, A.; Marín-Hernández, C.; Moragues, M. E.; Sancenón, F.; Dingwall, P.; Brown, N. J.; Martínez-Mañez, R.; White, A. J. P.; Wilton-Ely, J. D. E. T. Ruthenium(II) and osmium(II) vinyl complexes as highly sensitive and selective chromogenic and fluorogenic probes for the sensing of carbon monoxide in air. *Chem. Eur. J.* **2015**, *21*, 14529-14538; c) Marín-Hernández, C.; Toscani, A.; Sancenón, F.; Wilton-Ely, J. D. E. T.; Martínez-Mañez, R. Chromo-fluorogenic probes for carbon monoxide detection. *Chem. Commun.* **2016**, *52*, 5902-5911.

(18) a) Cannadine, J. C.; Hill, A. F.; White, A. J. P.; Williams, D. J.; Wilton-Ely, J. D. E. T. Organometallic macrocycle chemistry. 5. σ-Vinyl and σ-aryl complexes of ruthenium(II) ligated by 1,4,7-trithiacyclononane: X-ray crystal structure of $[Ru(CH{=}CH_2)(CO)(PPh_3)([9]aneS_3)]PF_6{\cdot}2CH_2Cl_2$ *Organometallics* **1996**, *15*, 5409-5415; c) Hill, A. F.; White, A. J. P.; Williams, D. J.; Wilton-Ely, J. D. E. T. Polyazolyl chelate chemistry 8. Organometallic dihydrido bis(pyrazol-1-yl) borato complexes of ruthenium(II). *Organometallics* **1998**, *17*, 4249-4258; d) Wilton-Ely, J. D. E. T.; Pogorzelec, P. J.; Honarkhah, S. J.; Tocher, D. A. Mixed-donor ligands: Pyrrolecarbaldehyde and pyrrolecarbothioaldehyde σ-organyl complexes of ruthenium (II) and osmium (II). *Organometallics* **2005**, *24*, 2862-2874; e) Wilton-Ely, J. D. E. T.; Honarkhah, S. J.;Wang, M.; Tocher, D. A. σ-Organyl complexes of ruthenium and osmium supported by a mixed-donor ligand. *Dalton Trans.* **2005**, 1930-1939; f) Wilton-Ely, J. D. E. T.; Wang, M.; Honarkhah, S. J.; Tocher, D. A. Ruthenium hydride and vinyl complexes supported by nitrogen–oxygen mixed-donor ligands. *Inorg. Chim. Acta.* **2005**, *358*, 3218-3226; g) Wilton-Ely, J. D. E. T.; Wang,

M.; Benoit, D.; Tocher, D. A. Spectroscopic, Structural and Theoretical Investigation of Alkenyl Ruthenium Complexes Supported by Sulfur–Nitrogen Mixed-Donor Ligands. *Eur. J. Inorg. Chem.* **2006**, 3068-3078; h) Cowley, A. R.; Hector, A. L.; Hill, A. F.; White, A. J. P.; Williams, D. J.; Wilton-Ely, J. D. E. T. Synthesis and reactions of five-coordinate mono-and binuclear thiocarbonyl-alkenyl and thioacyl complexes of ruthenium(II). *Organometallics* **2007**, *26*, 6114-6125; i) Cowley, A. R.; Hector, A. L.; Hill, A. F.; White, A. J. P.; Williams, D. J.; Wilton-Ely, J. D. E. T. Synthesis and reactions of five-coordinate mono-and binuclear thiocarbonyl-alkenyl and thioacyl complexes of ruthenium(II). *Organometallics* **2007**, *26*, 6114-6125; j) Hill, A. F.; Jones, C.; White, A. J. P.; Williams, D. J.; Wilton-Ely, J. D. E. T. Mercuriophosphaalkene-P complexes: Crystal structure of $[Ru\{P(=CHBu^t)HgC_5H_4Fe(\eta\text{-}C_5H_5)\}Cl_2(CO)(PPh_3)_2]$. *J. Chem. Soc., Dalton Trans.* **1998**, 1419-1420; k) Bedford, R. B.; Hill, A. F.; Jones, C.; White, A. J. P.; Williams, D. J.; Wilton-Ely, J. D. E. T. Phosphaalkyne hydrometalation: Synthesis and reactivity of the complexes $[Ru(P{=}CHCMe_3)Cl(CA)(PPh_3)_2]$(A= O, S). *Organometallics* **1998**, *17*, 4744-4753.

(19) Jia, G.; Wu, W. F.; Yeung, R. C. Y.; Xia, H. P. Dimeric and polymeric ruthenium complexes with Ru-vinyl linkages. *J. Organomet. Chem.*, **1997**, *539*, 53-59.

(20) a) Aucott, S. M.; Milton, H. L.; Robertson, S. D.; Slawin, A. M. Z.; Woollins, J. D. The preparation and characterisation of bimetallic iridium(II) complexes containing derivatised bridging naphthalene-1,8-disulfur or 4,5-dithiolato acephenanthrylene ligands. *Dalton Trans.* **2004**, 3347-3352; b) Lang, R. F.; Ju, T. D.; Kiss, G.; Hoff, C. D.; Bryan, J. C.; Kubas, G. J. Oxidative addition of disulfides to the complex $W(CO)_3$(phen)(EtCN). Synthesis, structure, and reactivity of $W(CO)_2(phen)(SR)_2$ (R = Ph, Me, CH_2Ph, ^tBu; phen = 1,10-Phenanthroline) coordinatively unsaturated complexes of tungsten(II) that reversibly bind CO and other ligands. *Inorg. Chem.* **1994**, *33*, 3899-3907; c) Jessop, P. G.; Rettig, S. J.; Lee, C.-L.; James, B. R. Hydrido thiolato and thiolato complexes of ruthenium (II) carbonyl phosphines. *Inorg. Chem.* **1991**, *30*, 4617-4627; d) Markham, S. J.; Chung, Y. L.; Branum, G. D.; Blake, D. M. Reactions of iridium (I) compounds with oxidized derivatives of organic disulfides and with thionyl chloride. *J. Organomet. Chem.* **1976**, *107*, 121-127.

(21) a) Nuzzo, R. G.; Allara, D. L. Adsorption of bifunctional organic disulfides on gold surfaces. *J. Am. Chem. Soc.* **1983**, *105*, 4481–4483; b) Nuzzo, R. G.; Fusco, F. A.;

Allara, D. L. Spontaneously organized molecular assemblies. 3. Preparation and properties of solution adsorbed monolayers of organic disulfides on gold surfaces. *J. Am. Chem. Soc.* **1987**, *109*, 2358–2368; c) Chinwangso, P.; Jamison, A. C.; Lee, T. R. Multidentate adsorbates for self-assembled monolayer films. *Acc. Chem. Res.* **2011**, *44*, 511-519.

(22) a) Daniel, M.-C.; Astruc, D. Gold nanoparticles: assembly, supramolecular chemistry, quantum-size-related properties, and applications toward biology, catalysis, and nanotechnology. *Chem. Rev.* **2003**, *104*, 293-346; b) Beer, P. D.; Cormode, D. P.; Davis, J. J. Zinc metalloporphyrin-functionalised nanoparticle anion sensors. *Chem. Commun.* **2004**, 414–415; c) Cormode, D. P.; Davis, J. J.; Beer, P. D. Anion sensing porphyrin functionalized nanoparticles. *J. Inorg. Organomet. Polym.* **2008**, *18*, 32–40.

(23) a) Lewis, D. J.; Pikramenou, Z. Lanthanide-coated gold nanoparticles for biomedical applications. *Coord. Chem. Rev.* **2014**, *273*, 213–225; b) Beloglazkina, E. K.; Majouga, A. G.; Romashkina, R. B.; Zyk, N. V.; Zefirov, N. S. Gold nanoparticles modified with coordination compounds of metals: synthesis and application. *Russ. Chem. Rev.* **2012**, *81*, 65-90; c) Roy, S.; Pericàs, M. A. Functionalized nanoparticles as catalysts for enantioselective processes. *Org. Biomol. Chem.* **2009**, *7*, 2669-2677; d) Wilton-Ely, J. D. E. T. The surface functionalisation of gold nanoparticles with metal complexes. *Dalton Trans.* **2008**, 25-29.

(24) a) Gonzàlez de Rivera, F.; Angurell, I.; Rossell, O.; Seco, M.; Llorca, J. Organometallic surface functionalization of gold nanoparticles. *J. Organomet. Chem.* **2012**, *715*, 13-18; b) Friederici, M.; Angurell, I.; Rossell, O.; Seco, M.; Divins, N. J.; Llorca, J. Facile synthesis of palladium nanoparticles protected with alkanethiolates functionalized with organometallic fragments. *Organometallics* **2012**, *31*, 722−728; c) Friederici, M.; Angurell, I.; Rossell, O.; Seco, M.; Muller, G. Exploring palladium nanoparticles protected with alkanethiolates functionalized with organometallic units as potential catalysts for sequential reactions. *J. Mol. Catal. A: Chem.* **2013**, *376*, 7-12.

(25) a) Brust, M.; Walker, M.; Bethell, D.; Schiffrin, D. J.; Whyman, R. Synthesis of thiol-derivatised gold nanoparticles in a two-phase liquid–liquid system. *J. Chem. Soc., Chem. Commun.* **1994**, 801-802; b) Brust, M.; Fink, J.; Bethell, D.; Schiffrin, D. J.; Kiely, C. Synthesis and reactions of functionalised gold nanoparticles. *J. Chem. Soc., Chem. Commun.* **1995**, 1655-1656.

(26) Suoranta, T.; Niemelä, M.; Perämäki, P. Comparison of digestion methods for the determination of ruthenium in catalyst materials. *Talanta* **2014**, *119*, 425–429.

(27) a) Turkevich, J.; Stevenson, P. C.; Hillier, J. A study of the nucleation and growth processes in the synthesis of colloidal gold. *Discuss. Faraday Soc.* **1951**, *11*, 55–75; b) Grabar, K. C.; Freeman, R. G.; Hommer, M. B.; Natan, M. J. Preparation and characterization of Au colloid monolayers. *Anal. Chem.* **1995**, *67*, 735-743; c) Kimling, J.; Mier, M.; Okenve, B.; Kotaidis, V.; Ballot, H.; Plech, A. Turkevich method for gold nanoparticle synthesis revisited. *J. Phys. Chem.* **2006**, *110*, 15700-15707.

(28) a) Jadzinsky, P. D.; Calero, G.; Ackerson, C. J.; Bushnell, D. A.; Kornberg, R. D. Structure of a thiol monolayer-protected gold nanoparticle at 1.1 Å resolution. *Science* **2007**, *318*, 430-433; b) Heaven, M. W.; Dass, A.; White, P. S.; Holt, K. M.; Murray, R. W. Crystal structure of the gold nanoparticle $[N(C_8H_{17})_4][Au_{25}(SCH_2CH_2Ph)_{18}]$. *J. Am. Chem. Soc.* **2008**, *130*, 3754-3755.

(29) a) Akola, J.; Walter, M.; Whetten, R. L.; Häkkinen, H.; Grönbeck, H. On the structure of thiolate-protected Au_{25}. *J. Am. Chem. Soc.* **2008**, *130*, 3756-3757; b) Jiang, D.; Luo, W.; Tiago, M. L.; Dai, S. In search of a structural model for a thiolate-protected Au_{38} cluster. *J. Phys. Chem. C* **2008**, *112*, 13905-13910; c) Qian, H.; Eckenhoff, W. T.; Zhu, Y.; Pintauer, T.; Jin, R. Total structure determination of thiolate-protected Au_{38} nanoparticles. *J. Am. Chem. Soc.* **2010**, *132*, 8280–8281; d) Rojas-Cervellera, V.; Giralt, E.; Rovira, C. Staple motifs, initial steps in the formation of thiolate-protected gold nanoparticles: how do they form? *Inorg. Chem.* **2012**, *51*, 11422–11429; e) Naeem, S.; Serapian, S. A.; Toscani, A.; White, A. J. P.; Hogarth, G.; Wilton-Ely, J. D. E. T. Ring-closing metathesis and nanoparticle formation based on diallyldithiocarbamate complexes of gold(I): Synthetic, structural, and computational studies. *Inorg. Chem.* **2014**, *53*, 2404-2416.

(30) (a) Schmid, G.; Pfeil, R.; Boese, R.; Bandermann, F.; Meyer, S.; Calis, G. H. M.; Van der Velden, J. W. A. $Au_{55}[P(C_6H_5)_3]_{12}Cl_6$ - ein Goldcluster ungewöhnlicher Größe. *Chem. Ber.* **1981**, *114*, 3634-3642; (b) Schmid, G. Large clusters and colloids. Metals in the embryonic state. *Chem. Rev.* **1992**, *92*, 1709-1727; (c) Weare, W. W.; Reed, S. M.; Warner, M. G.; Hutchison, J. E. Improved synthesis of small ($d_{core} \approx 1.5$ nm) phosphine-stabilized gold nanoparticles. *J. Am. Chem. Soc.* **2000**, *122*, 12890-12891.

(31) a) Lu, X. M.; Yavuz, M. S.; Tuan, H. Y.; Korgel, B. A.; Xia, Y. N. Ultrathin gold nanowires can be obtained by reducing polymeric strands of oleylamine−AuCl

complexes formed via aurophilic interaction. *J. Am. Chem. Soc.* **2008**, *130*, 8900-8901; b) Ma, Y.; Zeng, J.; Li, W.; McKiernan, M.; Xie, Z.; Xia, Y. Seed-mediated synthesis of truncated gold decahedrons with a AuCl/oleylamine complex as precursor. *Adv. Mater.* **2010**, *22*, 1930-1934; c) Gomez, S.; Philippot, K.; Colliere, V.; Chaudret, B.; Senocq, F.; Lecante, P. Gold nanoparticles from self-assembledgold(I) amine precursors. *Chem. Commun.* **2000**, 1945-1946; d) Leff, D. V.; Brandt, L.; Heath, J. R. Synthesis and characterization of hydrophobic, organically-soluble gold nanocrystals functionalized with primary amines. *Langmuir* **1996**, *12*, 4723-4730.

(32) a) Selvam, T.; Chi, K.-M. Synthesis of hydrophobic gold nanoclusters: growth mechanism study, luminescence property and catalytic application. *J. Nanopart. Res.* **2011**, *13*, 1769–1780; b) Selvam, T.; Chi, K.-M.; Chiang, C.-M. Organic-phase synthesis of self-assembled gold nanosheets. *J. Nanopart. Res.* **2011**, *13*, 3275–3286.

(33) Tuchscherer, A.; Schaarschmidt, D.; Schulze, S.; Hietschold, M.; Lang, H. Simple and efficient: Gold nanoparticles from triphenylphosphane gold (I) carboxylates without addition of any further stabilizing and reducing agent. *Inorg. Chem. Comm.* **2011**, *14*, 676–678.

(34) a) Vignolle, J.; Tilley, T. D. N-Heterocyclic carbene-stabilized gold nanoparticles and their assembly into 3D superlattices. *Chem. Commun.* **2009**, 7230-7232; b) Collinson, J.-M.; Wilton-Ely, J. D. E. T.; Díez-González, S. Reusable and highly active supported copper (I)–NHC catalysts for Click chemistry. *Chem. Commun.* **2013**, *49*, 11358-11360.

(35) Landgraf, G. in *Gold - Progress in Chemistry, Biochemistry and Technology*; Schmidbaur, H., Ed.; John Wiley & Sons: Chichester, 1999.

(36) a) Corbierre, M. K.; Lennox, R. B. Preparation of thiol-capped gold nanoparticles by chemical reduction of soluble Au (I)-thiolates. *Chem. Mater.* **2005,** *17*, 5691-5696; b) Goulet, P. J. G.; Lennox, R. B. New insights into Brust− Schiffrin metal nanoparticle synthesis. *J. Am. Chem. Soc.* **2010**, *132*, 9582–9584; c) Simpson, C. A.; Farrow, C. L.; Tian, P.; Billinge, S. J. L.; Huffman, B. J.; Harkness, K. M.; Cliffel, D. E. Tiopronin gold nanoparticle precursor forms aurophilic ring tetramer. *Inorg. Chem.* **2010**, *49*, 10858–10866 d) Corbierre, M. K.; Beerens, J.; Lennox, R. B. Gold nanoparticles generated by electron beam lithography of gold(I)-thiolate thin films. *Chem. Mater.* **2005,** *17*, 5774-5779; e) Corbierre, M. K.; Beerens, J.; Beauvais, J.; Lennox, R. B. Uniform one-dimensional arrays of tunable gold nanoparticles with tunable interparticle distances. *Chem. Mater.* **2006,** *18*, 2628-2631.

(37) a) Nakamoto, M.; Yamamoto, M.; Fukusumi, M. Thermolysis of gold(I) thiolate complexes producing novel gold nanoparticles passivated by alkyl groups. *Chem. Commun.* **2002**, 1622–1623; b) Nakamoto, M.; Kashiwagi, Y.; Yamamoto, M. Synthesis and size regulation of gold nanoparticles by controlled thermolysis of ammonium gold(I) thiolate in the absence or presence of amines. *Inorg. Chim. Acta* **2005**, *358*, 4229–4236.

(38) Schmidbaur, H.; Schier, A. A briefing on aurophilicity. *Chem. Soc. Rev.* **2008**, *37*, 1931–1951.

(39) a) Nomiya, K.; Noguchi, R.; Sakurai, T. Synthesis and Crystal Structure of a Water-soluble Gold(I) Complex, $\{K_3[Au(mba)_2]\}_2$ Formed by 2-Mercaptobenzoic Acid (H_2mba), with Aurophilic Interaction in the Solid-State. *Chem. Lett.* **2000**, 274-275; b) Watase, S.; Nakamoto, M.; Kitamura, T.; Kanehisa, N.; Kai, Y.; Yanagida, S. Solid-state luminescence and crystal structures of novel gold(I) benzenethiolate complexes. *J. Chem. Soc.*, *Dalton Trans*. **2000**, 3585–3590.

(40) Quiros, I.; Yamada, M.; Kubo, K.; Mizutani, J.; Kurihara, M.; Nishihara, H. Preparation of alkanethiolate-protected palladium nanoparticles and their size dependence on synthetic conditions. *Langmuir* **2002**, *18*, 1413-1418.

(41) Bruce, M. I.; Horn, E.; Matisons, J. G.; Snow, M. R. Chemistry of the Group 1B metals. XVII. Preparation of some gold(I) acetylide complexes containing Group 5 donor ligands: Crystal and molecular structures of $Au(C_2C_6F_5)(PPh_3)$. *Aust. J. Chem.* **1984**, *37*, 1163-1170.

(42) Bailey, J. Tricyclohexylphosphinegold compounds. *J. Inorg. Nucl. Chem.* **1973**, *35*, 1921-1924.

(43) Schmidbaur, H.; Wohlleben, A.; Wagner, F.; Orama, O.; Huttner, G. Gold-Komplexe von Diphosphinomethanen, I. Synthese und Kristallstruktur zweikerniger Gold (I)-Verbindungen. *Chem. Ber.* **1977**, *110*, 1748-1754.

(44) Hill, D. T.; Girard, G. R.; McCabe, F. L.; Johnson, R. K.; Stupik, P. D.; Zhang, J. H.; Reiff, W. M.; Eggleston, D. S. [μ-1,1'-Bis(diphenylphosphino)ferrocene]bis(chlorogold): Synthesis, iron-57 and gold-197 Moessbauer spectroscopy, x-ray crystal structure, and antitumor activity. *Inorg. Chem.* **1989**, *28*, 3529-3533.

(45) de Fremont, P.; Scott, N. M.; Stevens, E. D.; Nolan, S. P. Synthesis and structural characterization of N-heterocyclic carbene gold (I) complexes. *Organometallics* **2005**, *24*, 2411-2418.

(46) a) Sullivan, B. P.; Meyer, T. J. Comparisons of the physical and chemical properties of isomeric pairs. Photochemical, thermal and electrochemical cis-trans isomerizations of $M(Ph_2PCH_2PPh_2)_2Cl_2$ (M = Ru^{II}, Os^{II}). *Inorg. Chem.* **1982**, *21*, 1037-1040; b) Keller, A.; Jasionka, B.; Glowiak, T.; Ershov, A.; Matusiak, R. Cyclic oxycarbene and vinylidene complexes of ruthenium with (P^P) and (N^N) type ligands. *Inorg. Chim. Acta* **2003**, *344*, 49-60.

(47) (a) Hill, A. F.; Melling, R. P. Diyne coordination chemistry: Reactions of $[RuClH(CO)(PPh_3)_3]$ with diphenylbutadiyne and bis(phenylethynyl)mercury. *J. Organomet. Chem.* **1990**, *396*, C22−C24; (b) Alcock, N. W.; Hill, A. F.; Melling, R. P. Polyazolyl chelate chemistry 3. (Sigma-organyl)[tris(pyrazol-1-yl)borato]ruthenium complexes. *Organometallics* **1991**, *10*, 3898−3903.

For Table of Contents:

Bifunctional chalcogen linkers for the stepwise generation of multimetallic assemblies and functionalized nanoparticles.

Jonathan A. Robson, Ferran Gonzàlez de Rivera, Khairil A. Jantan, Margot. N. Wenzel, Andrew J. P. White, Oriol Rossell, and James D. E. T. Wilton-Ely*

[ToC image]

A versatile dicarboxylic linker based on a disulfide unit is used to prepare a series of heteromultimetallic complexes incorporating between 2-7 transition metal centres, including examples with three different metals within the same molecular assembly. The same sulfur-oxygen linker provides a straightforward and versatile route to the immobilization of transition metal units on the surface of gold nanoparticles.

Supporting Information

Bifunctional chalcogen linkers for the stepwise generation of multimetallic assemblies and functionalized nanoparticles.

Jonathan A. Robson, Ferran Gonzàlez de Rivera, Khairil A. Jantan, Margot N. Wenzel, Oriol Rossell and James D. E. T. Wilton-Ely*

S.1 Selected NMR spectra

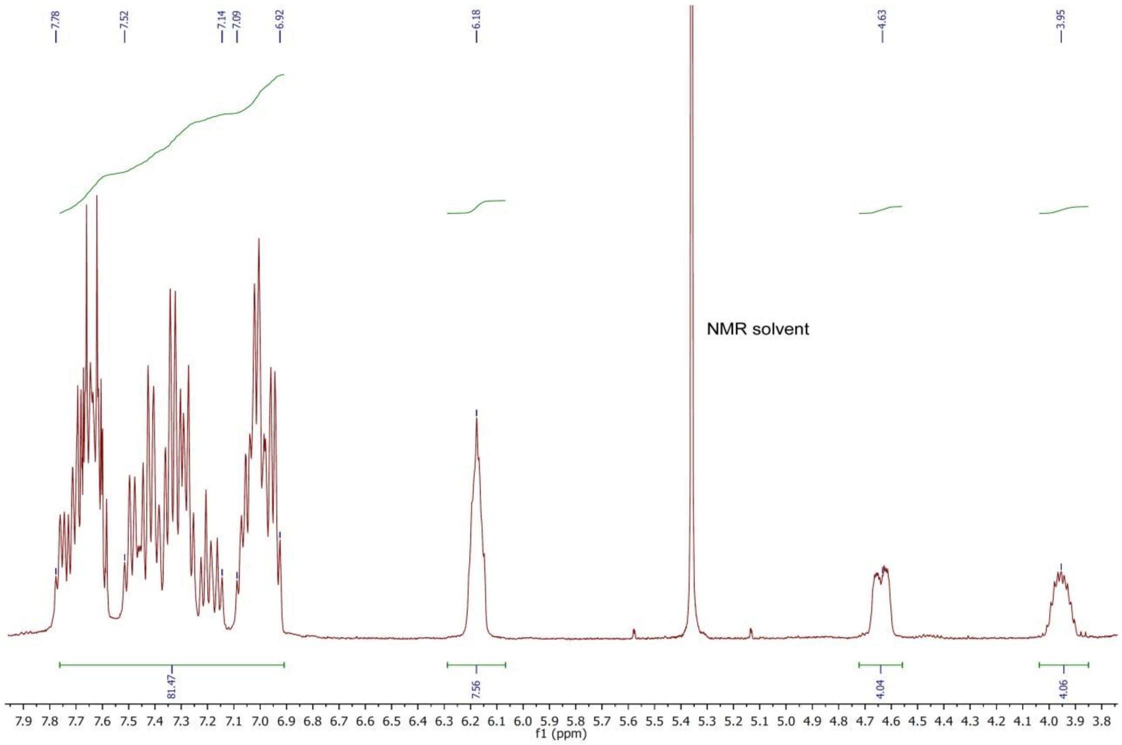

Fig. S1-1. ^{1}H NMR spectrum of $[\{Ru(dppm)_2(O_2CC_6H_4S\text{-}4)\}_2](PF_6)_2$ (**2**) in CD_2Cl_2 (spinning sidebands visible).

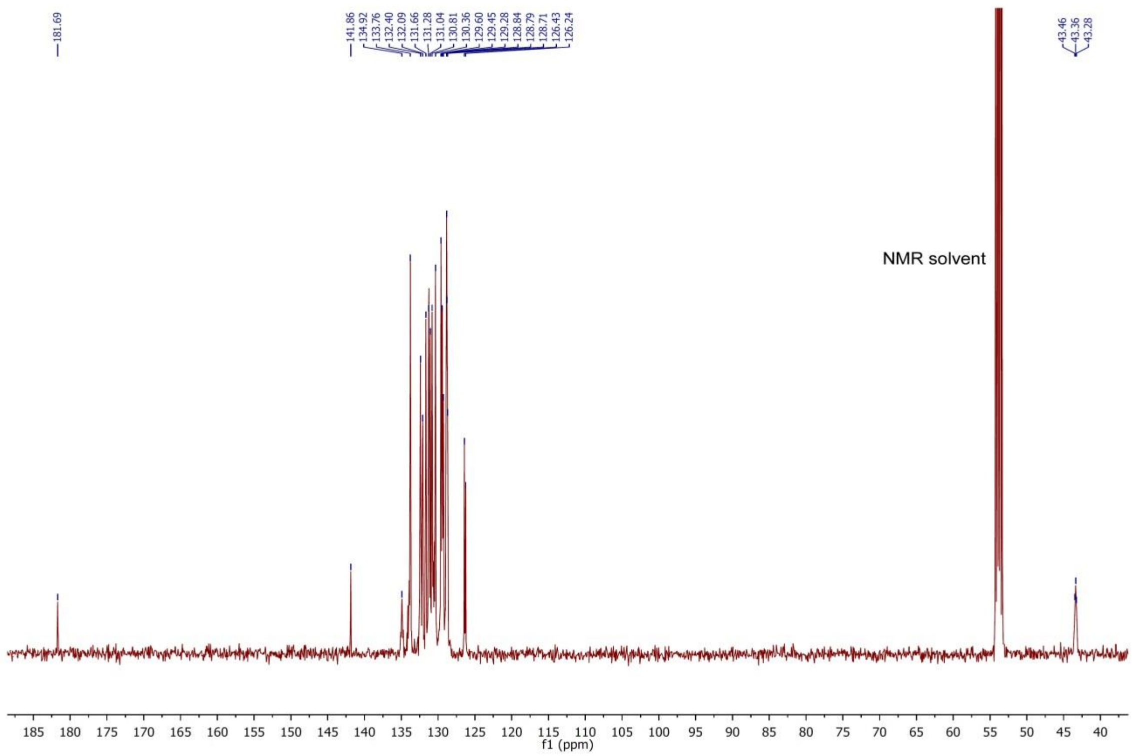

Fig. S1-2. $^{13}C\{^{1}H\}$ NMR spectrum of $[\{Ru(dppm)_2(O_2CC_6H_4S\text{-}4)\}_2](PF_6)_2$ (**2**) in CD_2Cl_2.

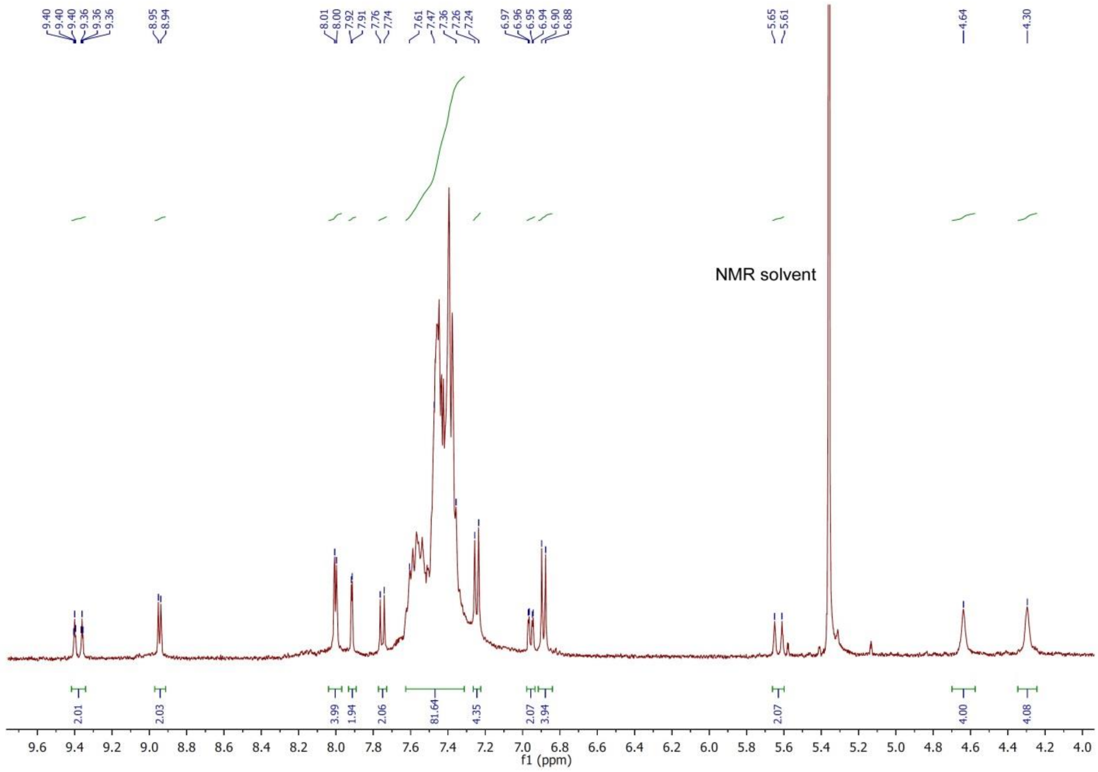

Fig. S1-3. [1]H NMR spectrum of [(dppf){$AuSC_6H_4CO_2Os$(CH=CH-bpyReCl$(CO)_3$)(CO)$(PPh_3)_2$}$_2$] (**15**) in CD_2Cl_2 (spinning sidebands visible).

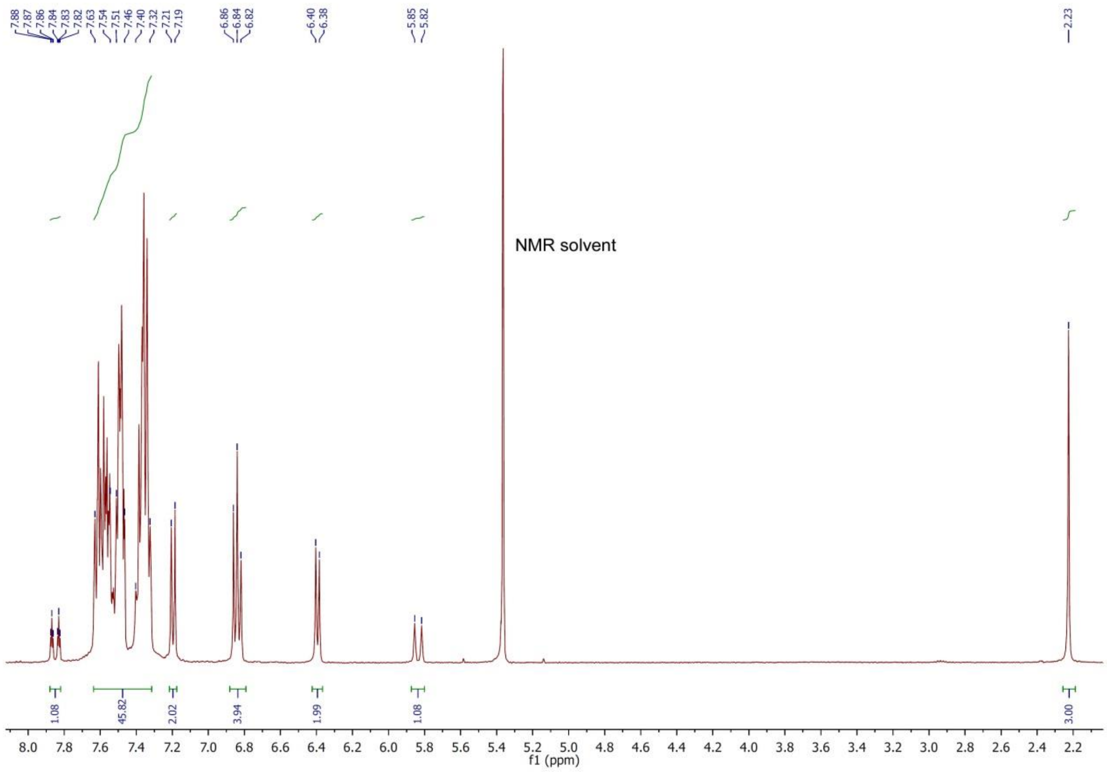

Fig. S1-4. [1]H NMR spectrum of [$(Ph_3P)Au(SC_6H_4CO_2$-4)Ru(CH=CHC_6H_4Me-4)(CO)$(PPh_3)_2$] (**16**) in CD_2Cl_2 (spinning sidebands visible).

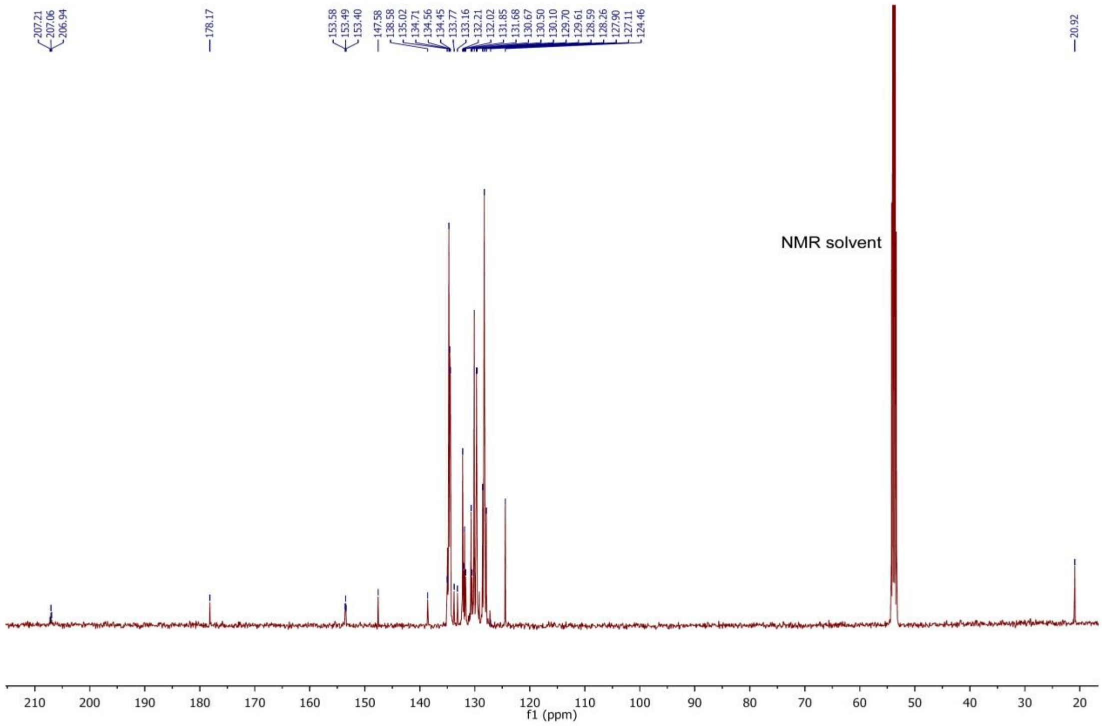

Fig. S1-5. $^{13}C\{^{1}H\}$ NMR spectrum of $[(Ph_3P)Au(SC_6H_4CO_2\text{-}4)Ru(CH{=}CHC_6H_4Me\text{-}4)(CO)(PPh_3)_2]$ (**16**) in CD_2Cl_2.

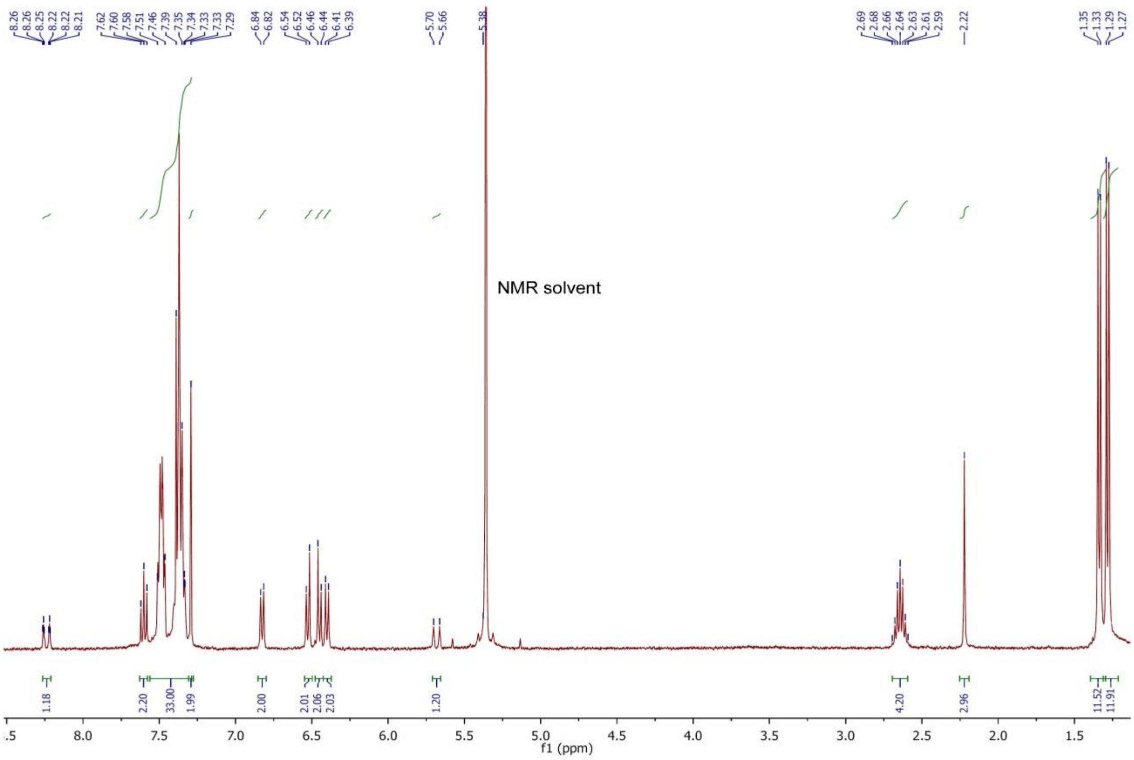

Fig. S1-6. ^{1}H NMR spectrum of $[(IDip)Au(SC_6H_4CO_2\text{-}4)Os(CH{=}CHC_6H_4Me\text{-}4)(CO)(PPh_3)_2]$ (**20**) in CD_2Cl_2 (spinning sidebands visible).

S.2 TEM, EDS and TGA data for NP1-NP4

General Comments. TEM images and EDS data were obtained at Imperial College using a JEOL 2010 high-resolution TEM (80-200 kV) equipped with an Oxford Instruments INCA EDS 80mm X-Max detector system. Thermogravimetric analysis was performed on a Mettler Toledo DSC 1LF/UMX Thermogravimetric Analyzer, using a platinum sample holder. The protocol used was to heat between 30-105 °C at 35 °C per minute then hold at 105 °C for 10 minutes before continuing to heat between 105-800 °C at 10 °C per minute. ICP-AES analyses were performed using a Perkin-Elmer 2000 DV ICP-OE spectrometer.

Analysis for $Au^{2.9}$@[$SC_6H_4CO_2Ru(dppm)_2$]PF_6 (NP1)

Transmission Electron Microscopy (TEM)

Average diameter 2.9 nm ± 0.2 based on over 200 nanoparticles.

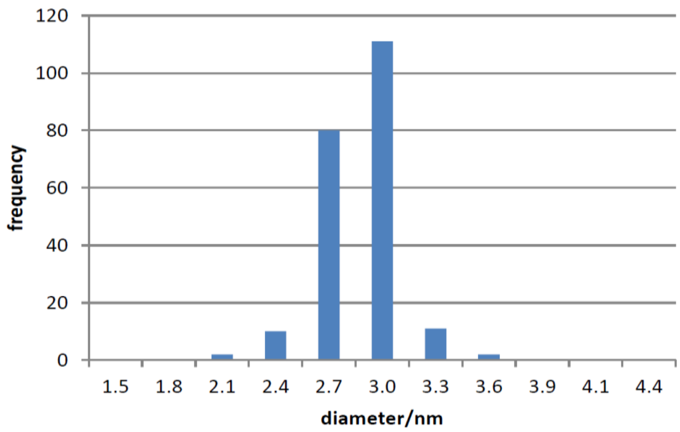

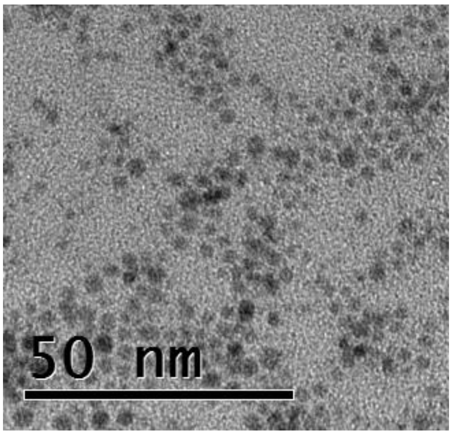

Energy dispersive X-ray spectroscopy (EDS)

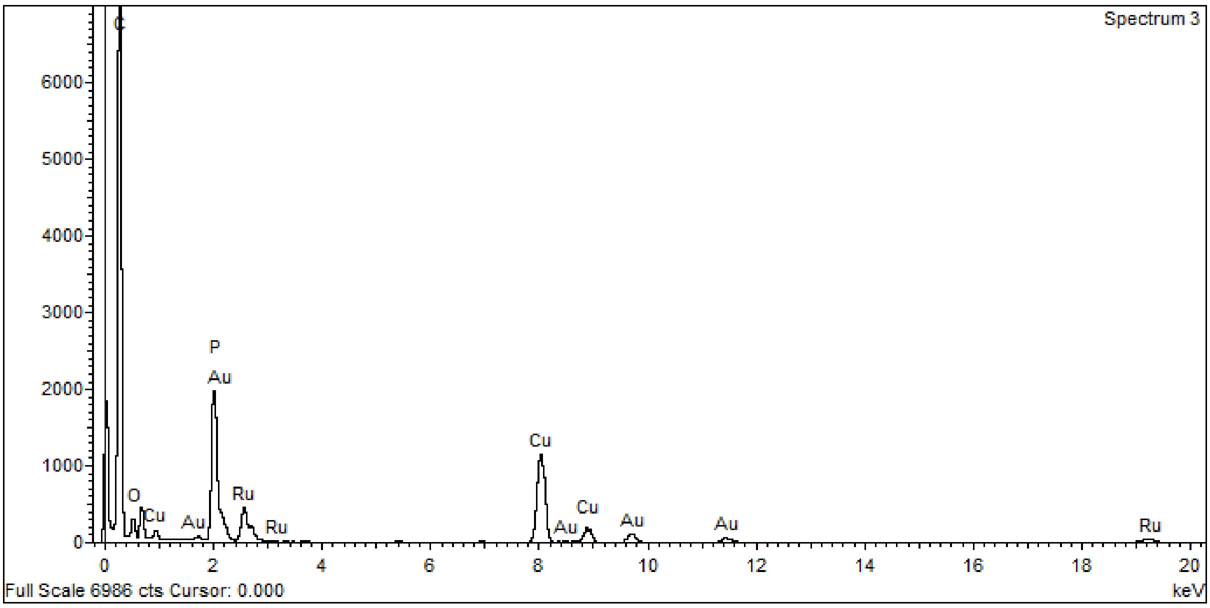

Confirms presence of Au and Ru. Presence of P/S and O/F indicated but not unambiguous.

Thermogravimetric analysis (TGA)

TGA was used to estimate the proportion of the mass attributable to the surface units. A sample of mass 1.530 mg of **NP1** was heated from 30 °C to 800 °C (total data points recorded in run: 4898). The reduction in mass was 37.8%, leaving gold and ruthenium metal (62.2%) as the only residue.

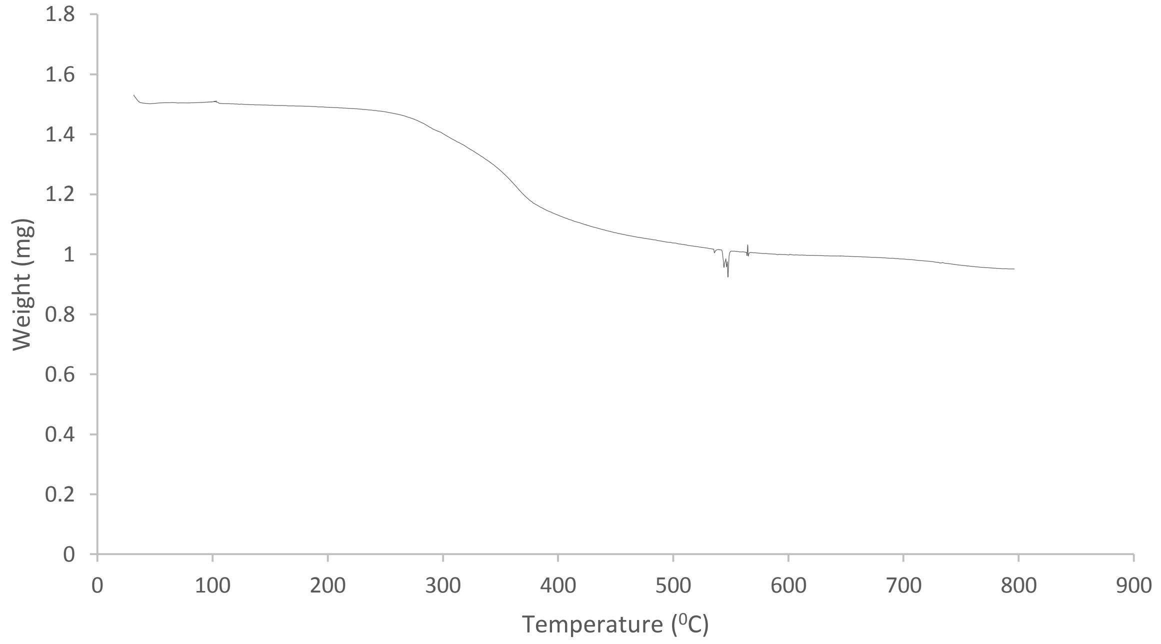

Analysis of Au$^{11.9}$@[SC$_6$H$_4$CO$_2$Ru(dppm)$_2$]PF$_6$ (NP2)

Transmission Electron Microscopy (TEM)

Average diameter 11.9 nm ± 0.9 based on over 200 nanoparticles.

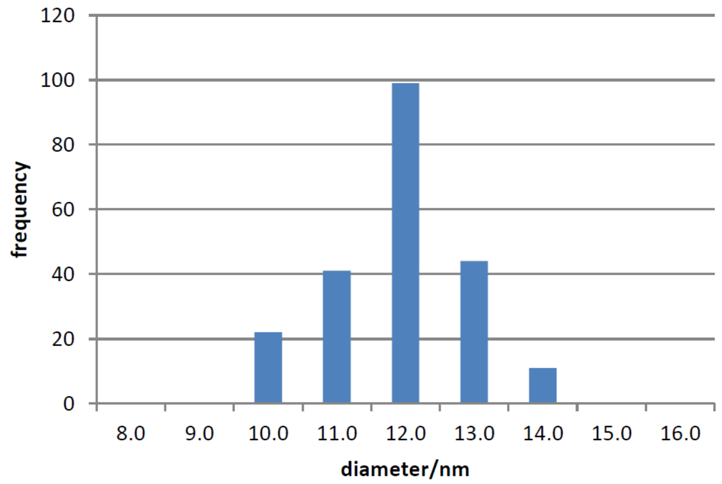

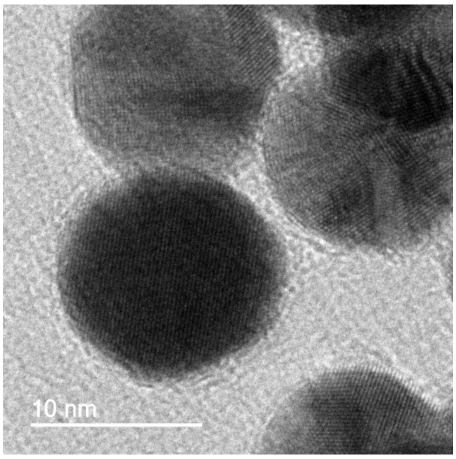

Energy dispersive X-ray spectroscopy (EDS)

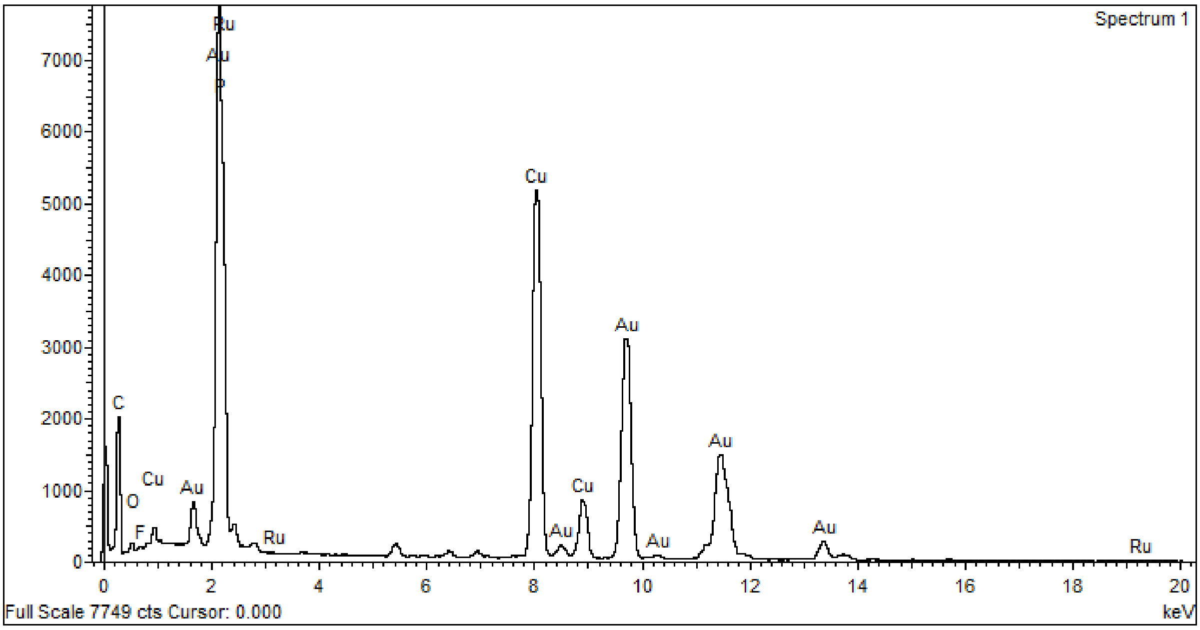

Confirms presence of Au and Ru. Presence of P/S and O/F indicated but not unambiguous.

Thermogravimetric analysis (TGA)

TGA was used to estimate the proportion of the mass attributable to the surface units. A sample of mass 0.779 mg of **NP2** was heated from 30 °C to 800 °C (total data points recorded in run: 4898). The reduction in mass was 42.5%, leaving gold and ruthenium metal (57.5%) as the only residue.

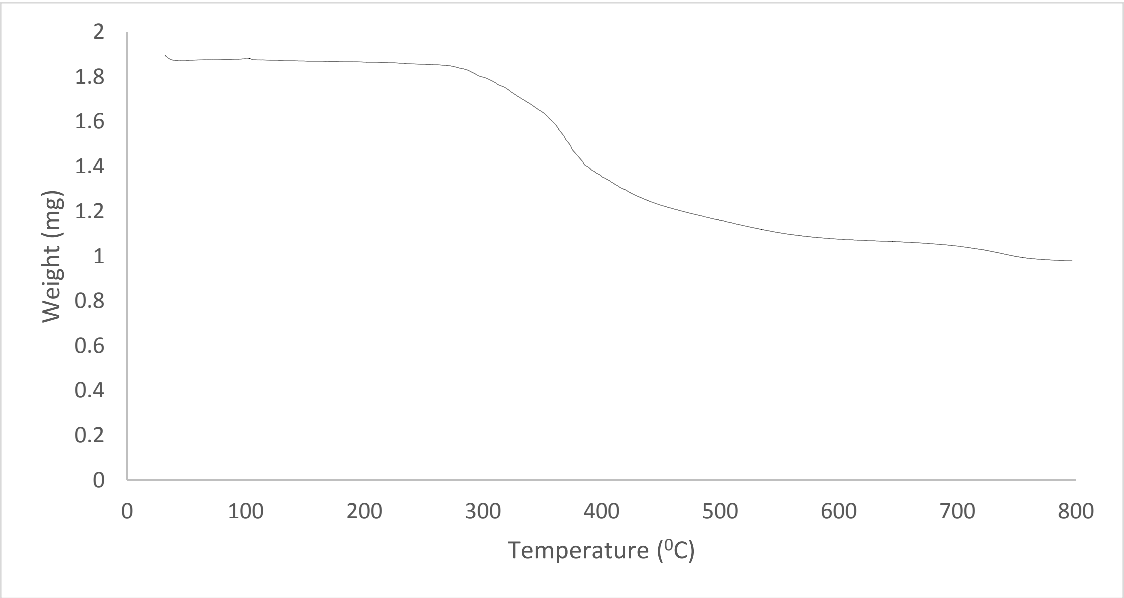

Analysis of $Au@SC_6H_4CO_2H$ (NP3)

Transmission Electron Microscopy (TEM)

Average diameter 4.1 nm ± 0.7 based on over 100 nanoparticles.

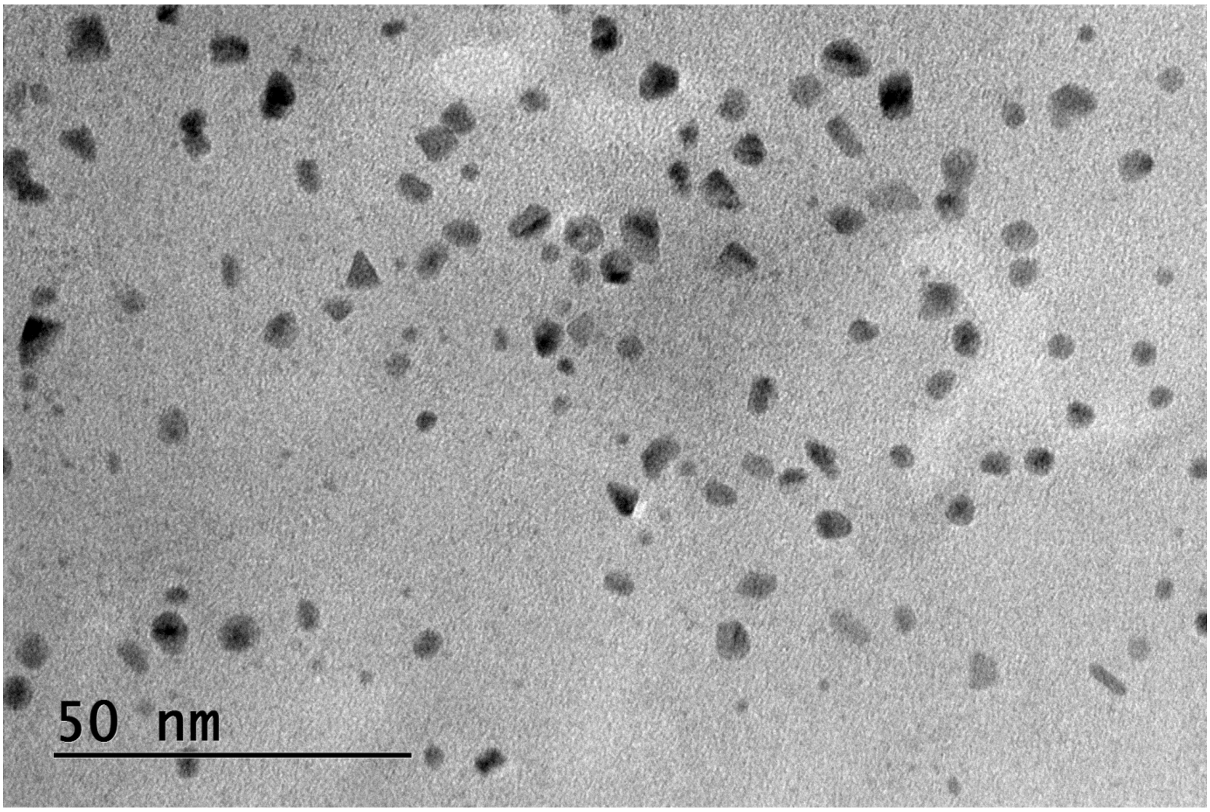

Energy dispersive X-ray spectroscopy (EDS)

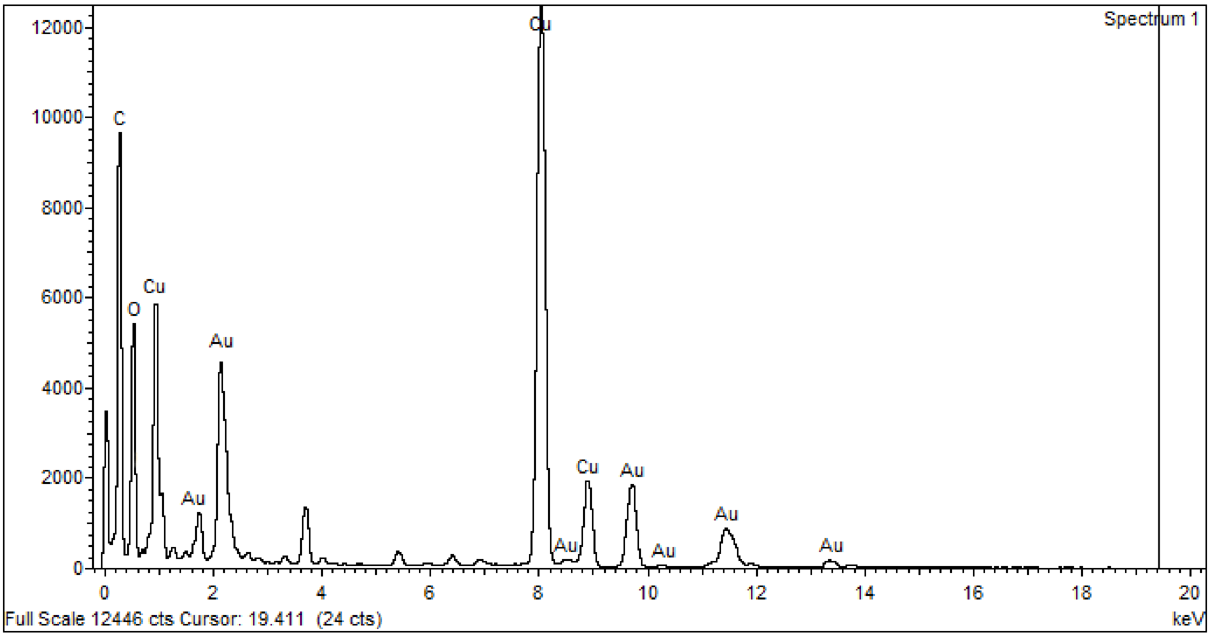

Analysis for $Pd@[SC_6H_4CO_2Ru(dppm)_2]PF_6$ (NP4)

Transmission Electron Microcopy (TEM)

Average diameter 2.2 nm ± 0.2 based on over 200 nanoparticles

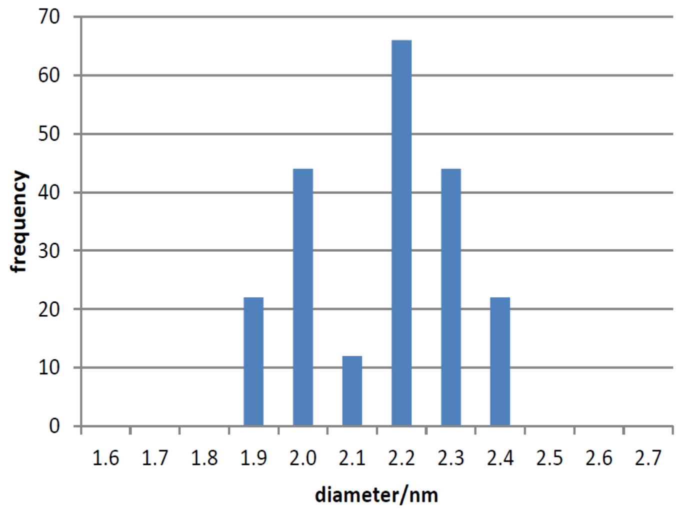

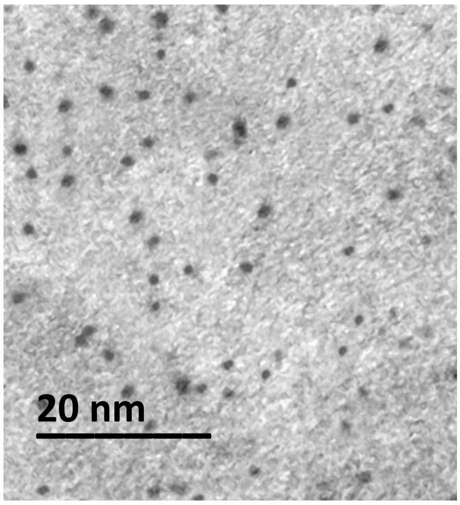

Energy dispersive X-ray spectroscopy (EDS)

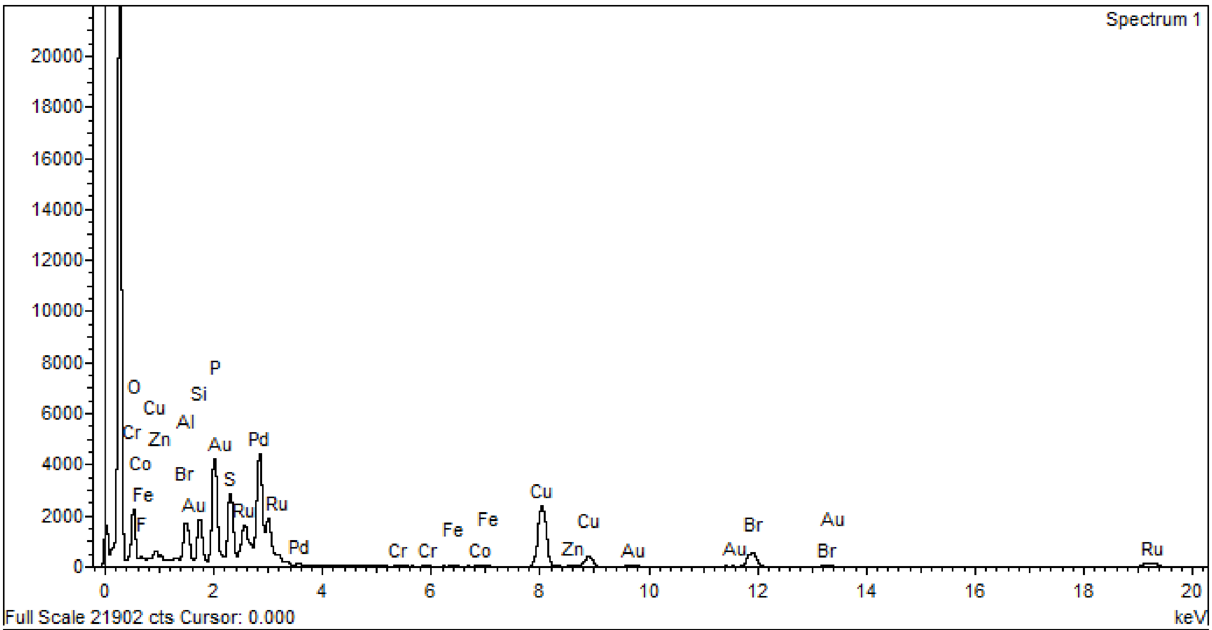

Confirms presence of Pd and Ru. Presence of P/S and O/F indicated but not unambiguous.

Thermogravimetric analysis (TGA)

TGA was used to estimate the proportion of the mass attributable to the surface units. A sample of mass 1.514 mg of **NP3** was heated from 30 °C to 800 °C (total points recorded in run: 4898). The reduction in mass was 38.4%, leaving palladium and ruthenium metal (61.6%) as the only residue.

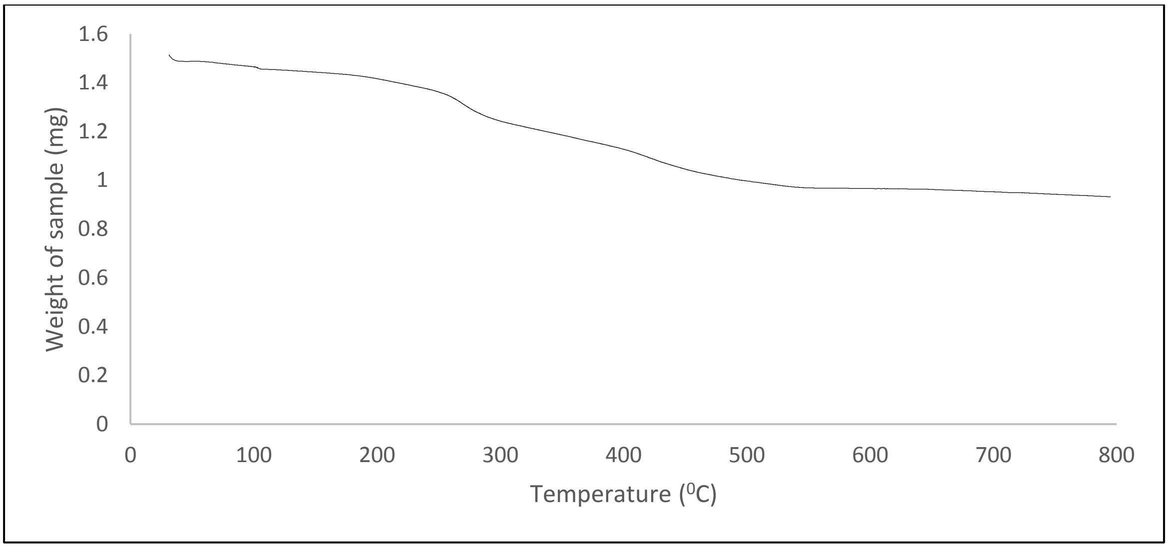

S.3 The Signer apparatus for molecular weight determination[S1-3]

The apparatus is shown below. Similar masses (10 mg) of the complex to be examined (‘unknown’) and a standard are weighed (to 4 decimal places) and dissolved, separately, in dichloromethane (~2-3 mL). These solutions are introduced to the separate bulbs of the apparatus and the taps closed. One valve is then attached to the Schlenk line and a very slight vacuum created. The apparatus is placed in a warm place and is left undisturbed while the vapour pressures equilibrate through the glass frit connecting the bulbs. To make the measurement, the apparatus is rotated so that the solvent fills the arms and the heights from the sealed end in both arms are determined. The heights of the solvent in the two arms will be proportional to the volume of solution. Readings are taken over a two day period until the measurements stabilise.

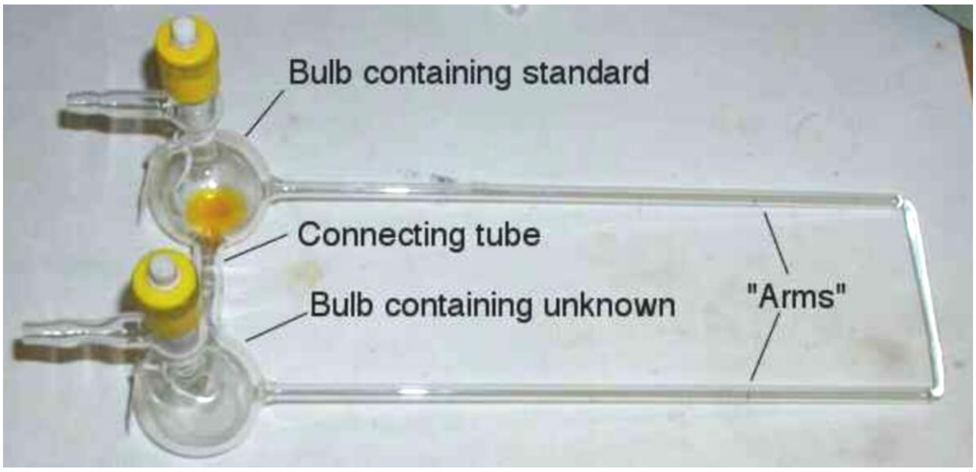

Fig. S3-1. The Signer apparatus for molecular weight determination.

Ferrocene (M_w = 186.03) is typically used as a standard, however, the standard should ideally have a similar molecular weight to the unknown being determined. For this reason, Vaska’s complex (M_w =780.25) was used for the determinations in this work. The stability of the standard in CD_2Cl_2 was confirmed by ^{31}P NMR spectroscopy over a period of days.

The molecular weight is then given by:

$$M_x = \frac{(m_x)(M_s)(h_s)}{(m_s)(h_x)}$$

Where:

M_x and M_s are the molar masses of the unknown and of the standard.

m_x and m_s are the masses of the unknown and of the standard used in the experiment.

h_x and h_s are the heights of the unknown and standard solutions in the arms.

S.4 Crystallography

The X-ray crystal structure of 21

Crystal data for **21**: $C_{77}H_{58}AuClN_2O_6P_3ReRuS \cdot 3.5(CH_2Cl_2)$, M = 2049.15, triclinic, P-1 (no. 2), a = 14.3062(4), b = 14.7789(5), c = 21.4417(6) Å, α = 70.190(3), β = 73.377(3), γ = 75.105(3)°, V = 4021.9(2) Å^3, Z = 2, D_c = 1.692 g cm^{-3}, μ(Mo-Kα) = 3.910 mm^{-1}, T = 173 K, orange blocks, Agilent Xcalibur 3E diffractometer; 15727 independent measured reflections (R_{int} = 0.0277), F^2 refinement,[S4] R_1(obs) = 0.0434, wR_2(all) = 0.1036, 11383 independent observed absorption-corrected reflections [$|F_o| > 4\sigma(|F_o|)$, $2\theta_{max}$ = 57°], 853 parameters. CCDC 1496662.

The mutually *trans* Cl1 chloride and C85/O85 carbonyl ligands bound to the rhenium center in the structure of **21** were found to be disordered, with a second orientation having the two ligands occupying exchanged positions. The geometries of the two orientations (of *ca*. 63 and 37% occupancy) were optimized and the thermal parameters of adjacent atoms were restrained to be similar. Only the atoms of the major occupancy orientation were refined anisotropically (those of the minor occupancy orientation were refined isotropically). Both the C51- and C76-associated phenyl rings were found to be disordered. In each case, two orientations were identified, of *ca*. 79:21 and 60:40% occupancy respectively. Their geometries were idealized, the thermal parameters of adjacent atoms were restrained to be similar, and only the non-hydrogen atoms of the major occupancy orientations were refined anisotropically (those of the minor occupancy orientations were refined isotropically).

The included solvent was found to be highly disordered and the best approach to handling this diffuse electron density was found to be the SQUEEZE routine of PLATON.[S5] This suggested a total of 286 electrons per unit cell, equivalent to 143 electrons per asymmetric unit. Before the use of SQUEEZE the solvent most resembled dichloromethane (CH_2Cl_2, 42 electrons), with 3.5 dichloromethane molecules corresponding to 147 electrons, so this was used as the solvent present. As a result, the atom list for the asymmetric unit is low by $3.5(CH_2Cl_2)$ = $C_{3.5}H_7Cl_7$ (and that for the unit cell is deficient by $C_7H_{14}Cl_{14}$) compared to what is actually presumed to be present.

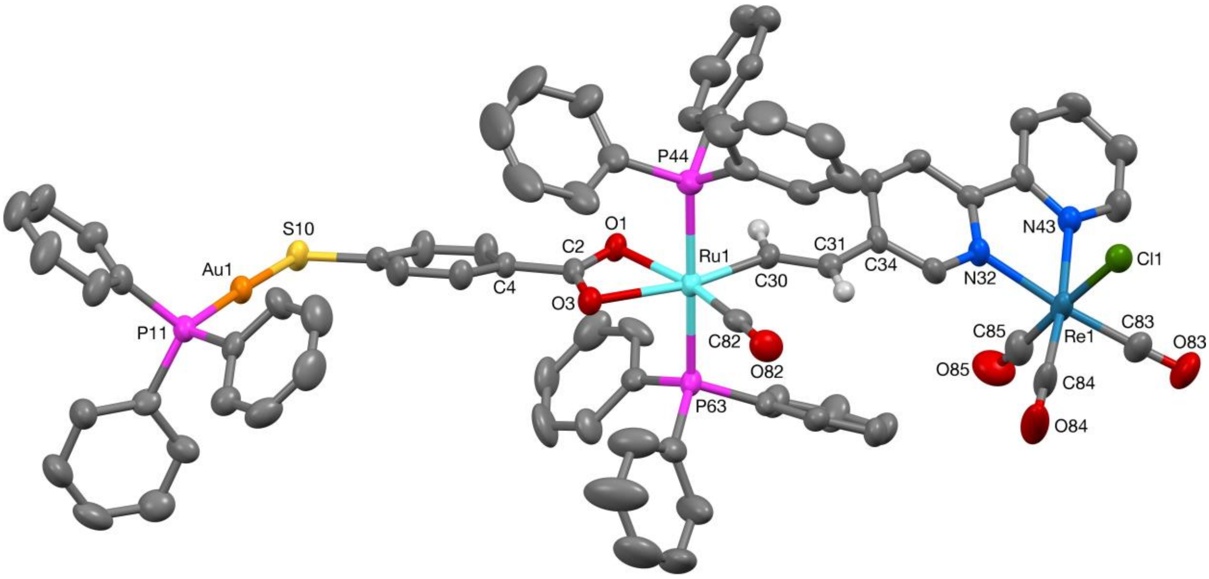

Fig. S4-1. The crystal structure of **21** (50% probability ellipsoids).

S.5 References

S1. Signer, R. *Annalen*, **1930**, *478*, 246.

S2. Clark, E. P. *Ind. Eng. Chem., Anal. Ed.* **1941**, *13*, 820.

S3. http://www.rsc.org/chemistryworld/Issues/2008/December/SignersOsmometer.asp

S4. (a) SHELXTL, Bruker AXS, Madison, WI; (b) SHELX-2013, Sheldrick, G. M. *Acta Cryst.* **2015**, *C71*, 3-8.

S5. Spek, A. L. (2003, 2009) PLATON, A Multipurpose Crystallographic Tool, Utrecht University, Utrecht, The Netherlands. See also Spek, A. L. *Acta. Cryst.*, **2015**, *C71*, 9-18.